NASA Contractor Report 172408

Final Technical Report FY 1982

Development of Powder Metallurgy 2XXX Series Al Alloys for High Temperature Aircraft Structural Applications

D. J. Chellman

LOCKHEED-CALIFORNIA COMPANY
BURBANK, CALIFORNIA 91520

CONTRACT NO. NAS1-16048
November 1984

National Aeronautics and
Space Administration

Langley Research Center
Hampton, Virginia 23665

NASA Contractor Report 172408

Final Technical Report FY 1982

Development of Powder Metallurgy 2XXX Series Al Alloys for High Temperature Aircraft Structural Applications

D. J. Chellman

LOCKHEED-CALIFORNIA COMPANY
BURBANK, CALIFORNIA 91520

CONTRACT NO. NAS1-16048
November 1984

National Aeronautics and
Space Administration

Langley Research Center
Hampton, Virginia 23665

1. Report No.	2. Government Accession No.	3. Recipient's Catalog No.
NASA CR - 172408		

4. Title and Subtitle	5. Report Date
DEVELOPMENT OF POWDER METALLURGY 2XXX SERIES Al ALLOYS FOR HIGH TEMPERATURE AIRCRAFT STRUCTURAL APPLICATIONS	2 NOVEMBER 1984
	6. Performing Organization Code
7. Author(s)	8. Performing Organization Report No.
D.J. CHELLMAN	LR 30322
	10. Work Unit No.
9. Performing Organization Name and Address	11. Contract or Grant No.
LOCKHEED - CALIFORNIA CO. P.O. BOX 551 BURBANK, CALIFORNIA 91520	NAS1 - 16048, MOD 8
	13. Type of Report and Period Covered
12. Sponsoring Agency Name and Address	15 AUGUST 1981 - 30 SEPTEMBER 1982
National Aeronautics and Space Administration Washington, DC 20546	14. Sponsoring Agency Code
	505-33-13-01

15. Supplementary Notes

NASA LANGLEY TECHNICAL CONTRACT MONITORS: S.M. DOLLYHIGH and W.B. LISAGOR, Jr.

16. Abstract

The objective of the present investigation was to improve the strength and fracture toughness combination of P/M 2124 Al alloys in accordance with NASA program goals for damage tolerance and fatigue resistance. Two (2) P/M compositions based on Al-3.70 Cu-1.85 Mg-0.20 Mn with 0.12 and 0.60 wt. pct. Zr were selected for investigation. The rapid solidification rates produced by atomization were observed to prohibit the precipitation of coarse, primary Al_3Zr in both alloys. A major portion of the Zr precipitated as finely distributed, coherent Al_3Zr phases during vacuum preheating and solution heat treatment. The proper balance between Cu and Mg contents eliminated undissolved, soluble constituents such as Al_2CuMg and Al_2Cu during atomization. The resultant extruded microstructures produced a unique combination of strength and fracture toughness. An increase in the volume fraction of coherent Al_3Zr, unlike incoherent $Al_{20}Cu_2Mn_3$ dispersoids, strengthened the P/M Al base alloy either directly by dislocation-precipitate interactions, indirectly by a retardation of recrystallization, or a combination of both mechanisms. Furthermore, coherent Al_3Zr does not appear to degrade toughness to the extent that incoherent $Al_{20}Cu_2Mn_3$ does. Consequently, the addition of 0.60 wt. pct. Zr to the base alloy, incorporated with a 774K (935°F) solution heat treatment temperature, produces an alloy which exceeds all tensile property and fracture toughness goals for damage tolerant and fatigue resistant applications in the naturally aged condition. These P/M 2124-Zr modified alloys display superior mechanical properties when compared to both other P/M 2124 Al alloys and an experimental I/M 2124 composition with 0.12 wt. pct. Zr.

17. Key Words (Suggested by Author(s))		18. Distribution Statement
Powder Metallurgy	Fracture Toughness	UNCLASSIFIED - UNLIMITED
2124 Al Alloys	Extrusion	
Damage Tolerance and Fatigue Resistance	Alloy Development	
High Temperature		

19. Security Classif. (of this report)	20. Security Classif. (of this page)	21. No. of Pages	22. Price*
UNCLASSIFIED	UNCLASSIFIED	56	

* For sale by the National Technical Information Service, Springfield, Virginia 22161

FOREWORD

This report documents the results of an on-going technical evaluation for the FY 1981/1982 time period that was performed by the Lockheed-California Company on advanced power metallurgy Al alloys. The reporting period is from 15 August 1981 through 30 September 1982. The research study was conducted for the NASA Advanced Supersonic Technology Project Office under NASA Contract NAS1-16048, Modification 8. S. M. Dollyhigh and W. B. Lisagor served as Technical Monitors on the present effort at the NASA-Langley Research Center.

The author is grateful to the extensive subcontract work performed by J. A. Walker, H. G. Paris and their associates at Aluminum Company of America's Technical Research Laboratory. The author is also grateful to G. G. Wald and I. F. Sakata for their technical contributions to this effort.

The author dedicates these research studies on P/M 2XXX series Al alloys to the memory of G. G. Wald whose passing was marked on 10 September 1982. He formulated the metallurgical basis for all Lockheed research and development activities in the P/M Al alloy development area and served continuously as a consulting metallurgist on the present research effort. His technical brilliance, disarming wit, and endless enthusiasm will be greatly missed by all of his colleagues.

Prior work conducted during FY 1980/1981 (16 July 1980 through 15 August 1981) by the Lockheed-California Company on this contract is reported by NASA Contractor Report 165965, entitled "Development of Powder Metallurgy 2XXX Series Al Alloys for High Temperature Aircraft Structural Applications - Phase II."

CONTENTS

LIST OF FIGURES

LIST OF FIGURES (Continued)

LIST OF TABLES

DEVELOPMENT OF POWDER METALLURGY 2XXX SERIES AL ALLOYS FOR HIGH TEMPERATURE AIRCRAFT STRUCTURAL APPLICATIONS

D. J. Chellman

Lockheed-California Company

SUMMARY

The objective of the present investigation was to improve the strength and fracture toughness combination of P/M 2124 Al alloys in accordance with NASA program goals for damage tolerance and fatigue resistance. Two (2) P/M compositions based on Al-3.70 Cu-1.85 Mg-0.20 Mn with 0.12 and 0.60 wt. pct. Zr were selected for investigation. The rapid solidification rates produced by atomization were observed to prohibit the precipitation of coarse, primary Al_3Zr in both alloys. A major portion of the Zr precipitated as finely distributed, coherent Al_3Zr phases during vacuum preheating and solution heat treatment. The proper balance between Cu and Mg contents eliminated undissolved, soluble constituents such as Al_2CuMg and Al_2Cu during atomization. The resultant extruded microstructures produced a unique combination of strength and fracture toughness. An increase in the volume fraction of coherent Al_3Zr, unlike incoherent $Al_{20}Cu_2Mn_3$ dispersoids, strengthened the P/M Al base alloy either directly by dislocation-precipitate interactions, indirectly by a retardation of recrystallization, or a combination of both mechanisms. Furthermore, coherent Al_3Zr does not appear to degrade toughness to the extent that incoherent $Al_{20}Cu_2Mn_3$ does. Consequently, the addition of 0.60 wt. pct. Zr to the base alloy, incorporated with a 774K (935°F) solution heat treatment temperature, produces an alloy which exceeds all tensile property and fracture toughness goals for damage tolerant and fatigue resistant applications in the naturally aged condition. These P/M 2124-Zr modified alloys display superior mechanical properties when compared to both other P/M 2124 Al alloys and an experimental I/M 2124 composition with 0.12 wt. pct. Zr.

SYMBOLS, ABBREVIATIONS, ACRONYMS

Symbol	Definition	SI Units	Customary Engineering Units
AA	artificially aged	-	-
APD	average powder diameter	-	-
E_c	modulus of elasticity in compression	GPa	Msi
E, E_t	modulus of elasticity in tension	GPa	Msi
ε	engineering strain	m/m	in/in
$\bar{\varepsilon}$	effective extrusion strain	non-dim	non-dim
$\dot{\varepsilon}$	time-average strain rate	mm/mm-sec	in/in-sec
G.P. (B) Zones	pre-precipitation clusters of Cu atoms on Al cube planes	-	-
Hi-Cu	high copper	-	-
Hi-Mn	high manganese	-	-
Hi-Zr	high zirconium	-	-
hr	hour	-	-
HM	high elastic modulus	-	-
HS	high strength	-	-
ΔK	stress intensity factor range	MPa-$m^{\frac{1}{2}}$	ksi-$in^{\frac{1}{2}}$
K_{app}	apparent plane stress fracture toughness	MPa-$m^{\frac{1}{2}}$	ksi-$in^{\frac{1}{2}}$
K_c	critical stress intensity factor	MPa-$m^{\frac{1}{2}}$	ksi-$in^{\frac{1}{2}}$
K_Q	stress intensity factor associated with experimental testing (5 pct. secant value)	MPa-$m^{\frac{1}{2}}$	ksi-$in^{\frac{1}{2}}$
K_r	stress intensity factor associated with experimental testing (25 pct. secant value)	MPa-$m^{\frac{1}{2}}$	ksi-$in^{\frac{1}{2}}$
K_{SC}	stress concentration factor	-	-
NA	naturally aged	-	-
NTS	notched tensile strength	MPa	ksi
NTS/YS	notched tensile strength to yield strength ratio	non-dim	non-dim
PA	artificially aged to peak strength condition	-	-
R	minimum to maximum fatigue stress factor	-	-
RA	reduction in area	percent	percent
ρ	density	-	-

Symbol	Definition	SI Units	Customary Engineering Units
SEM	scanning electron microscopy	-	-
SHT, ST	solution heat treatment	-	-
σ	engineering stress	MPa	ksi
s, sec	seconds	-	-
S	Al_2CuMg intermetallic precipitate equilibrium phase	-	-
S'	Al/Cu/Mg transition phase	-	-
θ	Al_2Cu intermetallic precipitate equilibrium phase	-	-
θ'	Al/Cu transition phase	-	-
θ''	ordered 2nd step G.P. zone formation (G.P. II)	-	-
TEM	transmission electron microscopy	-	-
TMT	thermomechanical treatment	-	-
WQ	water quench	-	-
w/o, wt. pct.	weight percent	-	-
YS	yield strength (0.2% offset)	MPa	ksi

1. INTRODUCTION

1.1 Objectives

The general objective of the FY1981/1982 structures/materials technology studies is to identify and conduct the research and development activities necessary to support decisions related to plans for future United States commercial air transportation. A major portion of the technology studies are focused on the development and evaluation of advanced Al alloy materials. Since 1979 Lockheed has been involved in the development of a family of advanced Al alloys in conjunction with several Al alloy producers. The research efforts have been directed toward the identification, fabrication, and characterization of a family of powder metallurgy (P/M) Al alloys tailored to satisfy specific design properties, including high strength, damage tolerance and fatigue resistance, high modulus, and low density. The goal is to realize Al alloys that exhibit specific strengths comparable to Ti alloys for supersonic cruise applications in the temperature range of 250° to 350°F. The technical approach has involved the implementation of alloying and processing systems that offer potential improvements in elevated temperature behavior over conventional Al alloys. New Al alloys are of interest for higher performance commercial aircraft structures because of their relatively low cost and ease of fabrication compared to alternative alloy materials.

The alloy development work reported herein covers the FY1981/1982 research efforts undertaken for achieving the damage tolerant and fatigue resistant target objectives given in table 1. Research activities in coordination with the Aluminum Company of America (ALCOA) addressed the application of P/M processing methods and alloy content modifications within the 2XXX series Al alloy system. Ingot metallurgy (I/M) alloy materials based on 2XXX series or Al-Cu-Mg alloys have been extensively used in naturally aged tempers for damage tolerant and fatigue resistant structural applications at room temperature. However, the necessity of elevated temperature service dictates the employment of artificially aged tempers where the strength, fracture toughness, and notched fatigue property combination available with I/M Al alloys are relatively poor. Alloy development studies on two (2) previous NASA-LaRC contracts have demonstrated that significant improvements in fracture toughness and notched fatigue properties are obtained by the fabrication of 2XXX series Al alloys with P/M processing techniques. The technical effort for this reporting period included the following research activities:

- Preparation of two P/M 2124 Al alloy type extruded bars based on Zr content modifications
- Determination of solution treatment, stretch, and age hardening behaviors of candidate P/M Al alloy extrusions by tensile screening tests
- Evaluation of size, shape, and distribution of Al_3Zr dispersoid phases using microanalytical techniques

TABLE 1. - FOUR (4) CATEGORIES OF TARGET OBJECTIVES FOR ADVANCED ALUMINUM ALLOY DEVELOPMENT PROGRAM (1)

Requirements	High Strength - Corrosion Resistance A		High Strength - Corrosion Resistance B		Damage Tolerance - Fatigue Resistance		High Stiffness		Low Density	
1. Strength: F_{tu}-MPa (ksi)	579	(84)	517	(75)	479	(68)	427	(62)	427	(62)
F_{cy}-MPa (ksi)	558	(82)	503	(73)	427	(62)	379	(55)	379	(55)
2. Fatigue:* F_{max}-MPa (ksi)	159	(23)	145	(21)	206	(30)	131	(19)	131	(19)
**ΔK -MPa$\sqrt{m}$ (ksi$\sqrt{in.}$)	6.82	(6.2)	6.16	(5.6)	7.92	(7.2)	6.16	(5.6)	6.16	(5.6)
3. Fracture Toughness: K_{App}-MPa$\sqrt{m}$ (ksi$\sqrt{in.}$)	66	(60)	66	(60)	89.1	(81)	66	(60)	66	(60)
K_{Ic}-MPa$\sqrt{m}$ (ksi$\sqrt{in.}$)	28.6	(26)	28.6	(26)	33	(30)	28.6	(26)	13.8	(12.5)
4. Density: ρ-grams/cm^3 (lb/in.^{3})	2.79	(.101)	2.50	(.09)	--	--	--	--	2.50	(.09)
5. Elastic Modulus: E-Pa (msi)	72.5	(10.5)	85.4	(12.4)	73.7	(10.7)	***90.3	(13.1)	86.1	(12.5)
6. Corrosion Resistance:										
Stress Corrosion -MPa (ksi)	172	(25)	172	(25)	172	(25)	172	(25)	172	(25)
Exfoliation Corrosion	>EA	>EA	>EA	>EA	>EA	>EA	>EA	>EA	>EA	>EA

*F_{max} at 10^5 cycles, K_t = 3, R = 0.1
**ΔK for R = 0.1, da/dn~10^{-6} m/m (in./in.)
*** Specific modulus (E/ρ)

Notes: Goal A represents target properties for Al alloys with conventional alloy density
Goal B represents target properties for low density Al alloys
Elevated temperature property goals include
a) Stability - room temperature properties unaffected by exposure up to 350°F
b) Greater than 80 pct. of room temperature properties in range of 250° to 350°F

- Assessment of influence of Zr additions on grain structure, recrystallization, and texture of P/M Al alloy extrusions
- Establish strength-fracture toughness property combination available with comparable I/M and P/M Al alloys
- Re-evaluation of P/M 2219 MOD Al alloy behavior in terms of higher solution treatment temperature
- Determination of long time exposure and stability properties for P/M 2124 Al alloys produced in Phase II study
- Comparison of candidate P/M 2XXX Al alloys with respect to achievement of damage tolerant and fatigue resistant objectives

1.2 Background

The achievement of improved property combinations for Al alloys applicable to supersonic aircraft structures has been demonstrated on two previous NASA-LaRC research programs by employing alloy modifications and P/M processing, Ref. 1 and 2. For damage tolerant and fatigue resistant goals (table 1), an attractive combination of tensile strength, fracture toughness, and fatigue properties was displayed by P/M composition variations based on 2124, 2618, and 2219 type Al alloys. In particular, research activities in cooperation with ALCOA have demonstrated the outstanding strength-toughness relationship available with extruded P/M 2XXX series Al alloys. The following problem areas were identified in the previous studies with respect to attainment of the damage tolerant and fatigue resistant target objectives: (1) low strength levels for P/M 2618 and 2219 Al alloys at room temperature, (2) reduction of fracture toughness in P/M 2618 and 2124-Hi Mn alloys, (3) loss of notched fatigue strengths in artificially aged tempers, and (4) degradation of elevated temperature and stability properties for P/M 2XXX series Al alloys at 350°F. These property results suggest that a complex compositional relationship exists between precipitate and dispersoid strengthening, elevated temperature environments, and fracture toughness considerations.

The Al-Cu-Mg alloys based on the 2124 type Al alloy composition presently demonstrate the most promising property combinations with respect to the damage tolerant and fatigue resistant goal. For this reason, the primary objective of the present study is to explore an improvement in strength and fracture toughness properties by employing alloy modifications to eliminate incoherent dispersoid and undissolved soluble constituent phases. Recent alloy development studies in the literature indicate that Zr additions are particularly effective in contributing to a fine grained and unrecrystallized microstructure in Al alloy extrusions. The effect of work content and heat treatment condition on property combinations is certain to be as important for the candidate P/M 2124-Zr modified alloys as in previous Lockheed studies. A re-examination of the potential for P/M 2219 or Al-Cu alloys to meet target goals was undertaken by using an optimum solution heat treatment schedule.

2. EXPERIMENTAL PROCEDURE

2.1 Material Selection

The two Al alloy compositions based on Zr modifications, 514041 and 514042, were designed to eliminate undissolved soluble constituents and incoherent dispersoids in the Al-Cu-Mg alloy system. The equilibrium solvus diagram was used to select the maximum Cu and Mg content which allows full dissolution at the ternary eutectic temperature, 781K (946°F). A balance of Cu and Mg alloying contents in the ratio of 2.2/1.0 is known to yield stoichiometric Al_2CuMg or S phases. The melt composition was adjusted based on experience to account for Mg losses to oxidation during atomization, and for Cu and Mg losses to formation of Al_7Cu_2Fe and Mg_2Si insoluble phases. Precipitation of the incoherent dispersoid, $Al_{20}Cu_2Mn_3$ was avoided by maintaining the Mn content lower than the solid solubility limit at the vacuum preheat and solution heat treatment temperatures. Sufficient Mn was retained in solution to avoid the possibility of creating differences in the aging behavior between the new candidate P/M 2124/Zr modified alloys and P/M 2124 (designated 513708 and 513709). The compound Al_3Zr replaces $Al_{20}Cu_2Mn_3$ as the primary dispersoid phase. Two Zr solute levels, 0.14 and 0.70 wt. pct., were selected to determine the effect of exceeding the equilibrium solubility limit by a factor of five on the relative amounts of the incoherent, tetragonal and coherent, cubic Al_3Zr phases. The resultant influence of Zr content on wrought microstructures and mechanical properties will be evaluated with respect to program objectives. The target and melt compositions of the two P/M Al-Cu-Mg-Zr alloys, 514041 and 514042, are listed in table 2 along with the alloy contents investigated in previous NASA-LaRC funded research activities. The Cu/Mg ratios indicate that the actual powder chemistries are close to the required value for Al_2CuMg (S phase) and Al_2Cu(θ phase) precipitation hardened alloy systems. Compositions for the primary dispersoid forming element, namely Zr, are judged to be within acceptable limits. An I/M 2124 Al alloy containing Zr additions, designated 503315, was included in the present study to facilitate a direct comparison of the I/M and P/M processing on properties and microstructures.

The P/M 2XXX series Al alloy compositions from the Phase II Alloy Development Program were selected to correspond to I/M 2219 and 2618 type alloys. Alloy extrusions fabricated under this previous study will be subjected to additional mechanical property evaluations in the current research activity. The low Cu content 2219 Al alloy with approximately 0.3 wt. pct. Mg offers a potentially excellent combination of room temperature strength and elevated temperature properties. Two alloy selections were based on the 2618 Al alloy composition with a higher Cu target composition of 3.5 wt. pct., in order to improve the elevated temperature resistance. One of the high Cu content 2618 type alloys does not contain Fe and Ni additions. The Fe and Ni alloying modifications were omitted to determine the effect of dispersoid phases on damage tolerance and elevated temperature stability. The Si content was maintained at approximately 0.2 wt. pct. where the maximum influence on tensile properties is expected from literature data.

Approximately 300 pounds of irregularly shaped powder was produced at the ALCOA Technical Center for each candidate alloy composition. The atomization,

TABLE 2. - COMPOSITION OF P/M 2XXX SERIES AL ALLOYS DETERMINED FROM MELT SAMPLES

Program Phase	Sample No.		Alloy Content (wt. pct.)								
			Cu	Mg	Si	Fe	Ni	Mn	Zr	Zn	Cr
PM 2618	513707	Target	3.80	1.80	0.15	1.50	1.50	--	--	--	--
		Actual	3.80	1.93	0.07	1.53	1.73	0.01	--	--	--
PM 2124 - High Mn	513708	Target	4.00	1.60	--	--	--	1.50	--	--	--
		Actual	3.93	1.57	--	0.06	0.01	1.50	--	--	--
PM 2124 - Low Mn	513709	Target	4.00	1.60	--	--	--	0.50	--	--	--
		Actual	4.06	1.62	--	0.05	--	0.51	--	--	--
PM 2219	513887	Target	5.50	0.35	--	--	--	0.30	--	--	--
		Actual	5.19	0.38	0.12	0.06	--	0.18	--	--	--
PM 2618 - Mod A	513888	Target	3.50	1.65	0.20	1.20	1.10	--	--	--	--
		Actual	3.32	1.67	0.06	1.03	0.93	0.01	--	--	--
PM 2618 - Mod B	513889	Target	3.50	1.65	0.20	--	--	--	--	--	--
		Actual	3.19	1.67	0.24	0.07	--	0.01	--	--	--
PM 2124 - Low Zr	514041	Target	3.70	1.85	--	--	--	0.20	0.14	0.10	0.10
		Actual	3.73	1.81	0.02	0.04	0.01	0.14	0.12	0.08	0.01
PM 2124 - High Zr	514042	Target	3.70	1.95	--	--	--	0.20	0.70	0.10	0.10
		Actual	3.67	1.84	0.03	0.03	0.04	0.16	0.60	0.10	0.01
IM 2034	503315	Target	4.30	1.50	--	--	--	0.90	0.12	--	--
		Actual	4.36	1.56	0.07	0.06	0.00	0.90	0.10	0.01	0.00

consolidation, and fabrication schemes used to manufacture P/M extruded bar materials is identical to those employed in the previous investigations. A description of the P/M processing steps is given in the following section. Figure 1 shows the actual size distribution of the atomized powder and the average particle diameter determined by a Fisher subsieve sizer. These results indicate that the solidification rates characteristic of each alloy powder lot are similar during air atomization.

2.2 Materials and Specimen Preparation

The P/M processing steps employed in the conversion of air atomized powders to Al alloy extrusions were similar to those described in the two previous contract reports. Table 3 lists a description of the pertinent powder characteristics, consolidation, and billet fabrication conditions used to produce the P/M 2124-Zr modified alloys under evaluation in the current Phase III study. A 400 pound pot of the required melt composition was air atomized to recover at least 300 pounds of fine, irregular shaped powder with at least 85% by weight smaller than -325 mesh. The powder was screened through a 100 mesh sieve prior to cold isostatic pressing. Two 66 kg (145 lb) cold compacts of each alloy, 18.7 cm diameter (7.4 in.) by 109 cm long (42.9 in.), were formed in a wet bag system by isostatically pressing the powder at 207 MPa (30 ksi) to 75 percent of the alloy's theoretical density. The compacts were transferred into a 3003 Al canister, sealed, and vacuum preheated for approximately one hour at 20-40 μm pressure. Differential scanning calorimetry was used to identify the solvus and solidus temperatures. The program schedule did not allow completion of this task before the scheduled hot pressing date. Consequently, the hot pressing temperature, 777K (935°F), was chosen from the Al-Cu-Mg phase diagram to avoid equilibrium melting at the ternary eutectic, 781K (946°F). Proper selection of the vacuum preheat and hot pressing temperatures ensures both effective degassing and homogenization of the billet compact. The total heat-up cycle for hot pressing takes approximately 7 to 8 hours to complete. After the evacuation lines were sealed, the compacts were removed from the furnace and hot pressed at 621 MPa (90 ksi) to full density. The hot pressed P/M billet is 71.7 cm (28.2 in.) long from 21.4 cm diameter (8.4 in.) at the top, to 23.4 cm (9.2 in.) at the bottom in order to facilitate billet ejection from the hot pressing cylinder. The can material was removed by scalping the billet to 15.2 cm (6.0 in.) diameter and cutting 2.5 cm (1.0 in.) from each end. Additional 2.5 cm (1.0 in.) slices were cut off each end and saved for microstructural evaluation. Four 15.2 cm (6.0 in.) diameter by 33.0 cm (13.0 in.) long extrusion charges per alloy composition were made by sawing each billet in half.

The extrusion of P/M 2XXX Al alloys at 625K (666°F) necessitates the use of a shorter billet length to assure billet breakout. Breakout can occur at a higher temperature but leads to at least a 14 MPa (2 ksi) loss in strength levels. Consequently, the billets were cut in half to approximately 33.0 cm (13 in.) long and extruded to the minimum 2.5 cm (1.0 in.) butt length in order to reduce material loss. Four billets from each alloy composition were induction heated and extruded at a 12.5 to 1 reduction ratio into 1.9 cm x 8.9 cm x 305 cm (0.75 in. x 3.50 in. x 120 in.) bars. The ram speed, breakout

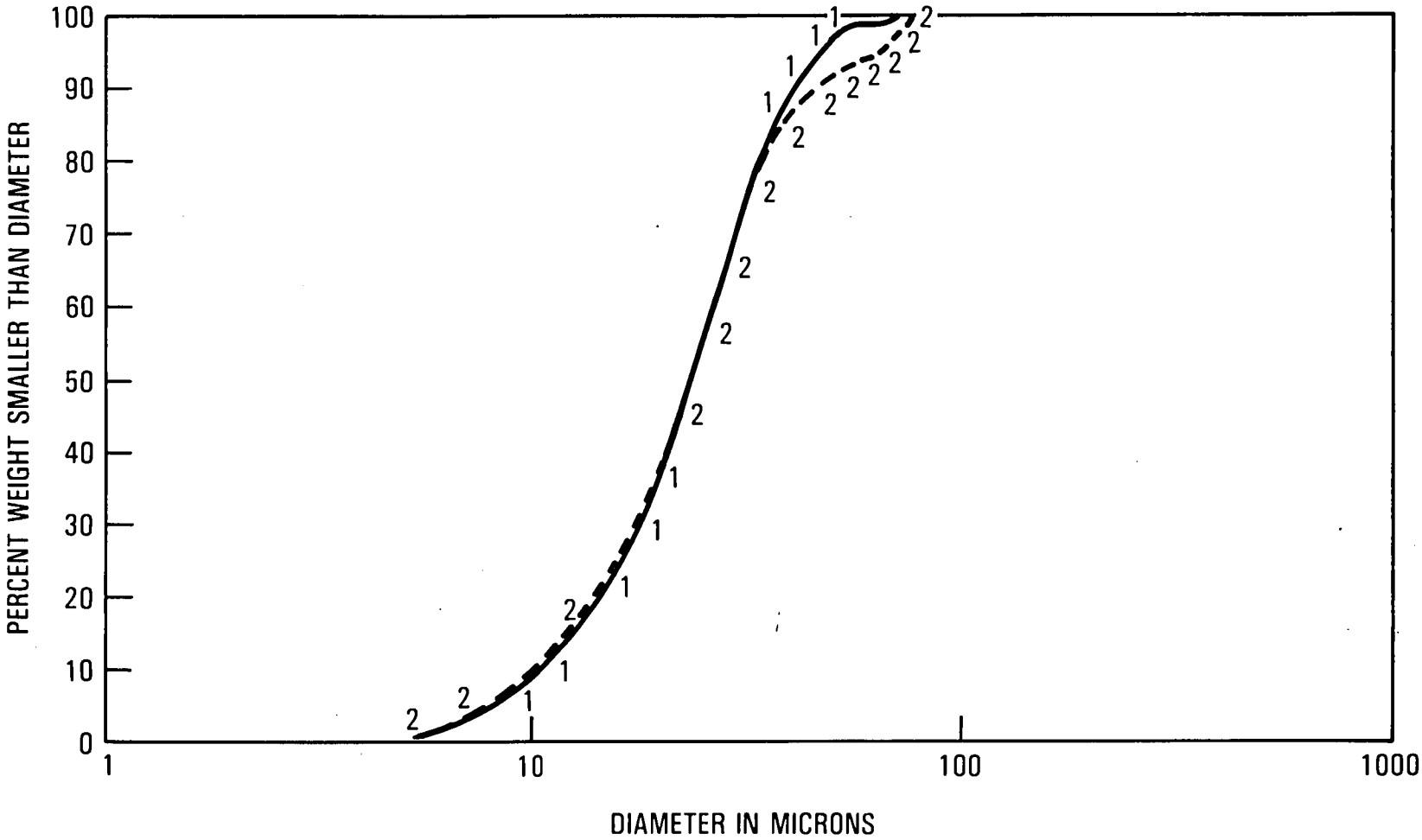

Figure 1. - The cumulative weight size distribution of 2124-Zr modified alloy 514041 and 514042 atomized powder shows that the physical characteristics of the two (2) alloys are nearly identical.

TABLE 3. - MANUFACTURING PARAMETERS OF ATOMIZED POWDERS, P/M AND I/M BILLETS, AND EXTRUSIONS

Sample No.	Powders A.P.D., μm	Billets (1) Vacuum Preheat (2) Temperature, K	Billets (1) Vacuum Preheat (2) Temperature, (°F)	Extrusions (3) Actual (4) Temperature, K	Extrusions (3) Actual (4) Temperature, (°F)	Extrusions (3) Solution Treatment Temperature, K	Extrusions (3) Solution Treatment Temperature, (°F)	Extrusions (3) Stress (5) Relief %
PM 2124-Low Zr-1	13.5	781.3	947	620.2	657	774.7	935	2.0
-2		781.3	947	607.4	634	774.7	935	2.0
-3		791.3	965	611.3	641	774.7	935	2.0
-4		791.3	965	610.8	640	774.7	935	2.0
PM 2124-High Zr-1	13.3	781.3	947	625.2	666	774.7	935	2.0
-2		781.3	947	625.2	666	774.7	935	2.0
-3		791.3	965	627.4	670	774.7	935	2.0
-4		791.3	965	625.8	667	774.7	935	2.0
IM 2034 -1	NA (6)	774.7	935(1)	666.3	740	774.7	935	2.0
-2	NA (6)	774.7	935(1)	669.1	745	774.7	935	2.0
PM 2219 -1	14.10	77.4	940	-----	---	802.4	985	2.0

Notes:
(1) Ingot preheated in air furnace.
(2) Actual compaction temperature is approximately 16.7K (30°F) lower.
(3) A constant ram speed of 3.3 cm/m (1.3 in/m) and butt length of 3.8 cm (1.5 in.) were used for all alloys.
(4) Temperature measured at rear of extrusion after butt was sheared off.
(5) Target Value.
(6) Not Applicable - Ingot.

and running pressures, and extrusion temperatures were identical to those used in the Phase II study. Speed-displacement curves indicated that the front 61 cm (24 in.) of the extrusions did not undergo steady state metal flow and thus they were scrapped.

All extrusions were solution heat treated at 775K (935°F) instead of 766K (920°F) to assure that the P/M 2124-Zr modified alloys were fully re-solution heat treated. Heating above the eutectic temperature, 781K (946°F), was avoided. After cold water quenching, the extrusions were stored in dry ice to retard natural aging. Gauge marks were scribed on the bar to assure accurate stress relief stretch measurements in the range of 1.5 to 2.0 pct. The P/M 2219 Al alloy extrusion was solution heat treated at a higher temperature of 802K (985°F) than used in the previous study. This thermal schedule was determined by DSC measurements and appears to be in agreement with the I/M 2219 processing data given in the literature. The extruded bars were subsequently stress relieved by 1.5 to 2.0 pct. stretch as performed on the other alloy materials.

2.3 Microstructural Examination

Metallographic specimens for optical microscopy, x-ray analysis, and transmission electron microscopy (TEM) were cut from the mid-length of the extrusions at the T/2, W/4 locations. Standard polishing procedures and Keller's reagent were used to reveal the grain structure. Transmission x-ray pinhole Laue patterns and pole figures were employed to identify intermetallic phases. TEM was used to provide structural information on the microstructural features that were unresolved by optical metallography and to identify the crystal structure, morphology, and size of Al_3Zr phases.

Crystallographic texture measurements were obtained from chemically thinned wafers representing the LT orientation. Intensity measurements from (111) diffraction were continuously collected between 0 and 60 degrees inclination to the specimen normal in 5 degree increments, with the sample rotated over 360° by 2 degree steps. The raw data were automatically corrected by a computer subroutine for adsorption before comparison to the intensity of a randomly textured Al standard. Pole figures were automatically plotted using intensity contours at 0.75, 1.25, 2.0, 3.0, and 4.0 times random. The maximum intensity within the pole figure is obtained by dividing any random intensity by the corresponding percentage provided on the plot.

Information on the crystallographic structure of the Al_3Zr phases was determined by selected area diffraction (SAD) and aperture limited microdiffraction. The compound Al_3Zr is known to exist in either the cubic $L1_2$ or tetragonal DO_{23} structure. The cubic $L1_2$ structure is coherent with the matrix and is identified by the presence of superlattice spots in the SAD patterns. The tetragonal, incoherent DO_{23} structure is identified by obtaining two (2) microdiffraction patterns with different zone axes. The angle between the zone axes was determined from the specimen stage rotation and tilt by measurement of the resultant angle on a Wolff net. The d spacings and interplanar angles for the tetragonal Al_3Zr phase were calculated using a programmable calculator, and the appropriate a_o and c_o values.

2.4 Testing Details

The mechanical testing objective of the current investigation was to determine the peak artificial aging practice for the alloys designated 513887, 514041, and 514042. The fracture toughness of these P/M Al alloys, as well as 513888 and 513889, were determined in the natural and peak aged tempers and compared to I/M 2124 Al alloy extrusions. The tensile and toughness specimens were machined and tested in accordance with ASTM standards. Smooth tapered seat 0.64 cm (0.25 in.) diameter tensile specimens were used in the aging study at 450K (350°F), 464K (375°F), and 478K (400°F) to determine the peak strength for various artificially aged tempers. The heat treatment results were subsequently used to age the full thickness L-T compact tension specimens. The K_Q values and R-curve analyses were used to establish a relative ranking of alloy behavior in the event that ASTM Method D399 criteria for plain strain fracture toughness were not satisfied. The room and elevated temperature tensile properties after 100, 1000, and 10,000 hours exposure at 394K (250°F) and 450K (350°F) were determined with 0.64 cm (0.25 in.) tapered seat and threaded end tensile specimens, respectively.

3. RESULTS AND DISCUSSION

3.1 Powder and Billet Microstructures

The fine, predominantly dendritic, structure of the irregularly shaped powder particles is similar to observations made in the two previous investigations. The 1 to 3 micron secondary dendritic arm spacing indicates that cooling rates from 10^3 to 10^5 K/sec were operative during the atomization process. A finer dendritic structure was typically observed in the P/M 2124-Zr modified alloys as a consequence of Zr additions to the base alloy. Cellular powder structures indicative of a substantially higher undercooling were occasionally observed. Table 4 lists the phases identified by Guinier phase analysis in the as-atomized powders. The volume fraction of phases is ranked semi-quantitatively by comparing the line intensity of a test film to that of an Al standard.

The presence of Al_2Cu detected in the two alloys is a result of solute segregation which creates the cored, mostly dendritic, structure. During solidification, solute is rejected from the solid, thereby progressively increasing the liquid solute content. The changing compositional path of the freezing liquid is described by the classical liquidus diagram. For alloys with Cu/Mg ratios greater and less than 2.2:1, the freezing liquid follows the path to the left and right of the quasi-binary hump, respectively,

$$Al_{\text{solid solution}} + Al_2Cu + Al_2CuMg.$$

If the solidification rate is sufficiently high, the solute can be retained in metastable, supersaturated solid solution. At lower solidification rates Al_2CuMg, Al_2Cu, and Mg_2Si may precipitate during the cool-down to ambient

TABLE 4. - PHASES IDENTIFIED IN P/M AND I/M 2XXX AL ALLOYS BY GUINIER X-RAY ANALYSIS

Sample No.	Product	Phases Present								
		$CuAl_2$	Al_2CuMg	θ'	S'	$Al_{20}Cu_2Mn_3$	Al_9FeNi	Al_7Cu_2Fe	Tetragonal Al_3Zr	Cubic Al_3Zr
PM 2618	Extrusion(1)	Trace	--	--	--	--	Med.	Med.	--	--
	Powder	--	V. Sml. -	--	--	--	Small +	--	--	--
PM 2124 - High Mn	Extrusion(1)	Small	--	--	--	Med.	--	--	--	--
	Powder	Small	V. Sml. -	--	--	Poss. Sml.	--	--	--	--
PM 2124 - Low Mn	Extrusion(1)	Small	--	--	--	Small	--	--	--	--
	Powder	Small	--	--	--	Small	--	--	--	--
PM 2124 - Low Zr	Extrusion(2)	--	--	--	--	--	--	V. Sml.	--	--
	Powder	V. Sml.	--	--	V. Sml. +	--	--	--	--	--
PM 2124 - High Zr	Extrusion(2)	--	--	--	--	--	--	--	Sml. +	Med. (3)
	Powder	V. Sml. +	--	--	V. Sml.	--	--	Trace	--	--
IM 2034	Extrusion(2)	--	V. Sml. +	--	--	Med.	--	V. Sml. -	--	--

Notes:
(1) Solution heat treated at 920°F, CWQ, stretched 1.5 - 2.0%, and naturally aged 4 days minimum.
(2) Solution heat treated at 935°F, CWQ, stretched 1.5 - 2.0%, and naturally aged 4 days minimum.
(3) Identified by TEM only. Quantity present is an estimated amount.

temperatures after solidification of the last portion of liquid phase at the eutectic composition. Rapid age hardening occurs in P/M Al alloys due to the promotion of rapid diffusion rates from the high concentration of quenched-in vacancies. Constituent phases that contain Mn, Fe, Ni, and Zr were not detected by Guinier analysis or metallographic examination of the as-polished powders at 1000X.

The microstructure of the candidate P/M billets was examined by optical metallography at 500X and 1000X. Guinier analysis of the phases present in the billets indicated that intermetallic compounds were detected that are similar to those observed in homogenized I/M 2024 billets. The advantage obtained by P/M processing involves the fine size and distribution of billet grains and intermetallic particles that are normally present as large constituents in I/M 2XXX Al alloys. The amount of primary soluble phases, Al_2Cu and Al_2CuMg, indicates that the segregation created during solidification is not completely eliminated by the precipitation and growth of intermetallic phases present in the atomized powder. The 1 hour holding time at 777K (935°F) during the vacuum preheating cycle may not be adequate to dissolve the large equilibrium Al_2Cu phases.

3.2 Extrusion Microstructures

The intermetallic phases, grain structure, and crystallographic texture which composes the microstructure of the P/M 2124-Zr modified extrusions are presented in the following sections. Metallographic results from the previous investigations are used where necessary to resolve the effect of compositional changes on property behavior in the current investigation. The phases identified in the naturally aged P/M 2XXX Al alloy and I/M 503315 extrusions are also listed in table 4. The calculated volume fraction of coherent Al_3Zr and incoherent $Al_{20}Cu_2Mn_3$ which precipitates at the vacuum preheat and solution heat treatment temperatures for alloys 503708, 513709, 514041, and 514042 are shown in table 5. Undissolved Al_2Cu in P/M 2124 (alloys 513708 and 513709) is eliminated by decreasing the Cu content as undertaken in alloys 514041 and 514042. Despite the occurrence of undissolved Al_2Cu in P/M 2124, coarse constituents such as Al_2CuMg in the I/M 503315 alloy are eliminated, as observed in figure 2. The incoherent dispersoid, $Al_{20}Cu_2Mn_3$ was not identified in either of the P/M 2124-Zr modified alloys. The absence of other Mn containing intermetallic phases indicates that most of the Mn was retained in solid solution.

The low Zr content of P/M 51401 and I/M 503315 made detection of Al_3Zr virtually impossible by Guinier X-ray techniques. At 775K (935°F) only 0.07 wt. pct. Zr is available for precipitation from solid solution, as opposed to 0.55 wt. pct. Zr in P/M alloy 514042, as approximated from the binary Al-Zr phase diagram given in figure 3. Tetragonal Al_3Zr and cubic Al_3Zr phases were detected only in the higher Zr content P/M 2124 Al alloy extrusions. The size and distribution of Al_3Zr can be controlled by the heating rate and preheat temperature. A decrease in the preheating rate from 50,000K/hr (90,000°F/hr) to less than 50K/hr (90°F/hr) has been reported to increase the recrystallization temperature of an I/M Al-Zn-Mg alloy containing 0.17 wt. pct. Zr by nearly 200K (360°F). The inhibition of recrystallization

TABLE 5. - CALCULATED HYPOTHETICAL VOLUME FRACTION OF DISPERSOIDS IN SEVERAL P/M 2XXX AL ALLOYS

Sample No.	Element (Wt. Pct.)	Dispersoid(1) Type	Estimated Volume Fraction (Pct.)
PM 2618	1.53 Fe, 1.73 Ni	Al_9FeNi, Al_7Cu_2Fe	10.51 (2)
PM 2124-High Mn	1.50 Mn	$Al_{20}Cu_2Mn_3$	4.99 (3)
PM 2124-Low Mn	0.51 Mn	$Al_{20}Cu_2Mn_3$	1.15 (3)
PM 2219	0.18 Mn	$Al_{20}Cu_2Mn_3$	0.0 (3)
PM 2618-Mod A	1.03 Fe, 0.93 Ni	Al_9FeNi,Al_7Cu_2Fe	6.71 (2)
PM 2618-Mod B	-----	-----	-----
PM 2124-Low Zr	0.12 Zr	Al_3Zr	0.09 (4)
PM 2124-High Zr	0.60 Zr	Al_3Zr	0.69 (4)

Notes: (1) Ignores Mg_2Si phase which is assumed to be present in the same amount in all P/M Al Alloys.

(2) Assumes no solid solubility, and that all excess Cu over 2.5 wt. pct. is used to form Al_7Cu_2Fe.

(3) Solubility is approximately 0.20 wt. pct. at 920°F.

(4) Solubility is approximately 0.07 wt. pct. at 935°F.

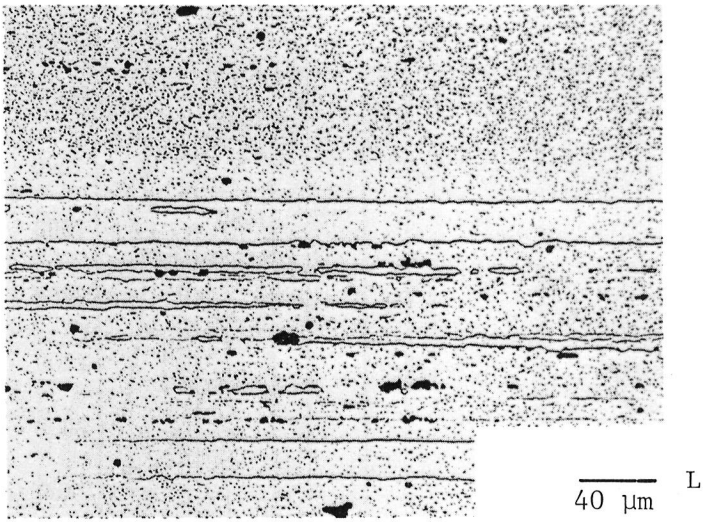

(a)

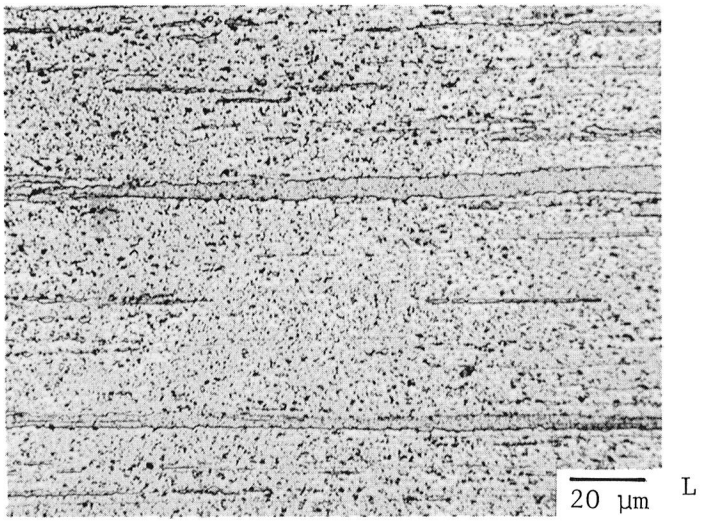

(b)

Figure 2. - Optical metallography showing the coarser microstructure of (a) I/M 503315 relative to (b) P/M 2124-Zr modified Al alloys.

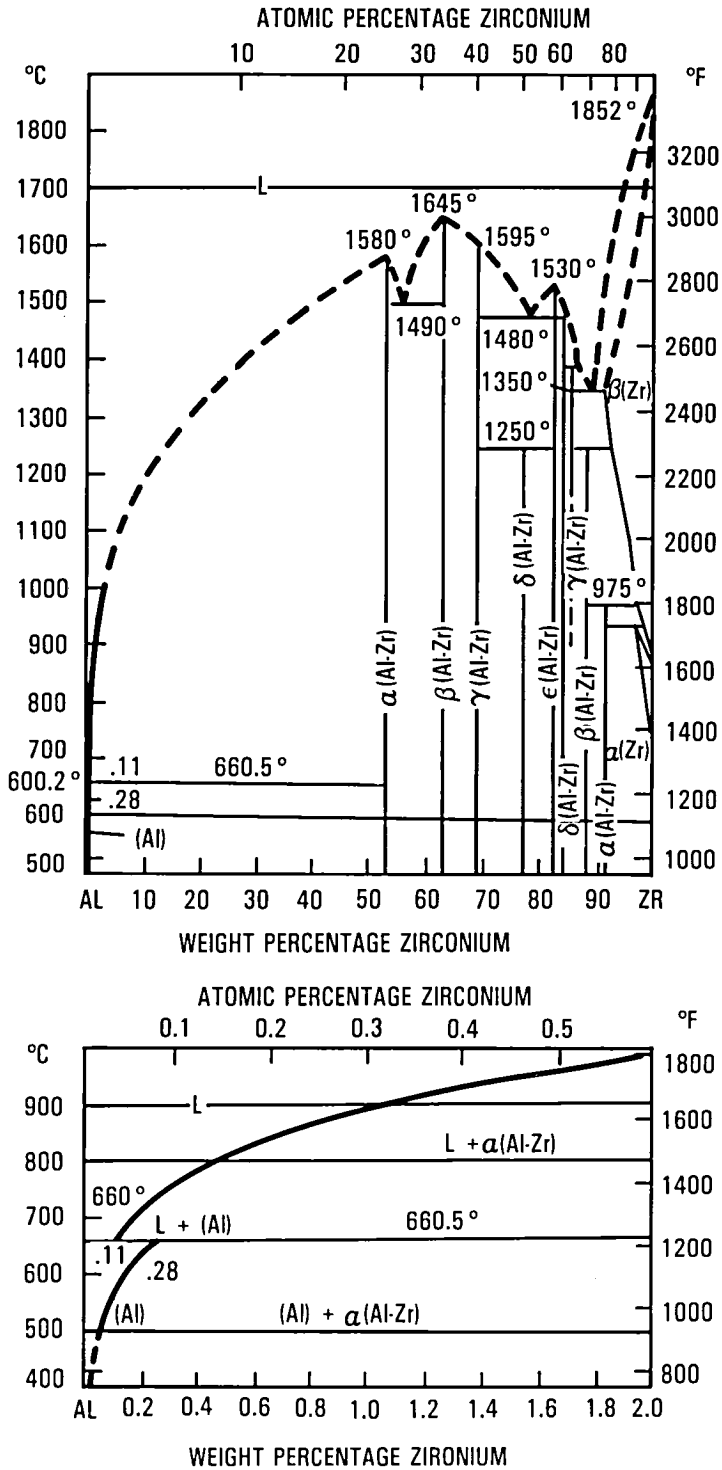

Figure 3. - The binary Al-Zr phase diagram showing the solid and liquid solubility of Zr at 774K (935°F).

mechanisms was explained by the presence of a fine, coherent Al_3Zr phase distribution, Ref. 3. Since the P/M compacts undergo a slow heating rate of approximately 10 to 20K/hr (18 to 36°F/hr) between 700K and 775K (800°F and 935°F) during the vacuum preheat cycle, a fine distribution of coherent Al_3Zr is expected. The copious precipitation of cubic Al_3Zr throughout the matrix of the PM Al alloy 514042 extrusion is shown by dark field imaging of a (100) superlattice spot in figure 4. Relative to $Al_{20}Cu_2Mn_3$ in P/M 2124 and Al_9NiFe and Al_7Cu_2Fe in alloy 513707, the Al_3Zr phase is much finer as evidenced in figures 5 and 6. Tetragonal Al_3Zr also occurs as coarser, more widely spaced rectangular shaped particles, typically less than 1.0 μm in length as given in figure 7. The diffraction patterns and crystallographic analysis used to identify the tetragonal Al_3Zr phase are described in the Appendix.

In conventionally cast ingot metallurgy alloys the Zr content is maintained below 0.12 wt. pct. to avoid formation of coarse, primary tetragonal Al_3Zr phases during solidification (figure 3). The absence of this phase in the as-atomized powder, as seen in table 4, indicates that tetragonal Al_3Zr in the P/M 2124-Zr modified 514042 extrusion forms either by precipitation from the solid solution (cubic to tetragonal transformation) or coarsening of fine, primary constituents which are undetectable by x-ray analysis techniques.

The grain structure of P/M 2124-Zr modified Al alloy extrusions is illustrated by the optical metallography in figure 8. The alloys are characterized by an extremely fine, elongated "pancake" grain structure which is very similar to P/M 2124 (figure 9). An increase in the Zr or Mn content of the respective alloys produces a finer grain structure. Relative to I/M 503315, little difference in structure exists between the two (2) P/M alloys. The grain structure of P/M produced 2XXX series Al alloys are at least an order of magnitude finer, as observed in figure 2.

The pinhole Laue patterns in figures 8 and 9 show that the P/M Al alloys possess a duplex texture characterized by a predominate (110) $[1\bar{1}2]$ sheet orientation which is representative of the unrecrystallized component, Ref. 4. Visual inspection of the relative intensity of (100) [100] diffraction spots for $\alpha = 48°$ on the (111) diffraction ring shows a qualitative difference in the degree of recrystallization between the two P/M Al alloys. A slightly higher (100) [001] spot intensity and greater degree of "spottiness" along the diffraction rings is observed for the P/M 2124 Al alloy containing 0.5 wt. pct. Mn (513709), with all other alloys being similar. In Al-Zn-Mg cold rolled sheet, the additions of 0.50 wt. pct. Mn and 0.21 wt. pct. Cr are not effective as recrystallization inhibitors, whereas the addition of 0.17 wt. pct. Zr increased the recrystallization temperature by nearly 200K (360°F), Ref. 3. The presence of Al_3Zr in the wrought P/M Al alloys appears to be only slightly more effective in inhibiting recrystallization and subgrain coalescence on an equal volume fraction basis.

The (111) pole figures in figure 10 were used to obtain a more accurate assessment of the P/M 2124-Zr modified crystallographic textures than available with pinhole Laue patterns. An increase in the volume fraction of cubic Al_3Zr resulted in an increase in the maximum intensity of the (110) $[1\bar{1}2]$ peak by approximately 28 percent and a decrease in the diffuse intensity

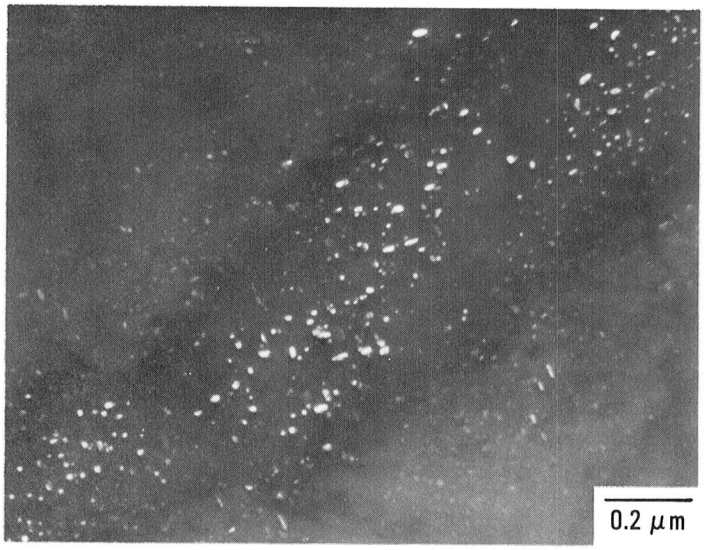

Dark Field Image (DF)

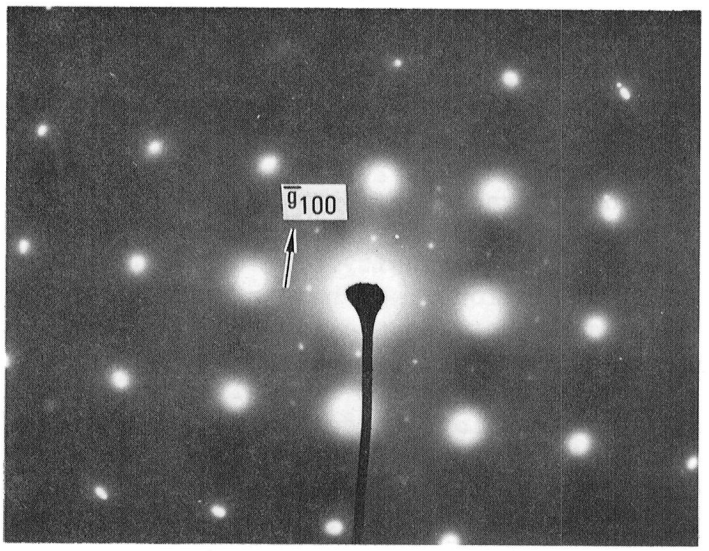

Selected Area Diffraction Pattern (SADP)

Figure 4. - Transmission electron microscopy (TEM) using dark field image of coherent $(L1_2)Al_3Zr$ dispersoid particles in alloy 514042. Image was formed by employing a $\bar{g}_{100}$ superlattice reflection.

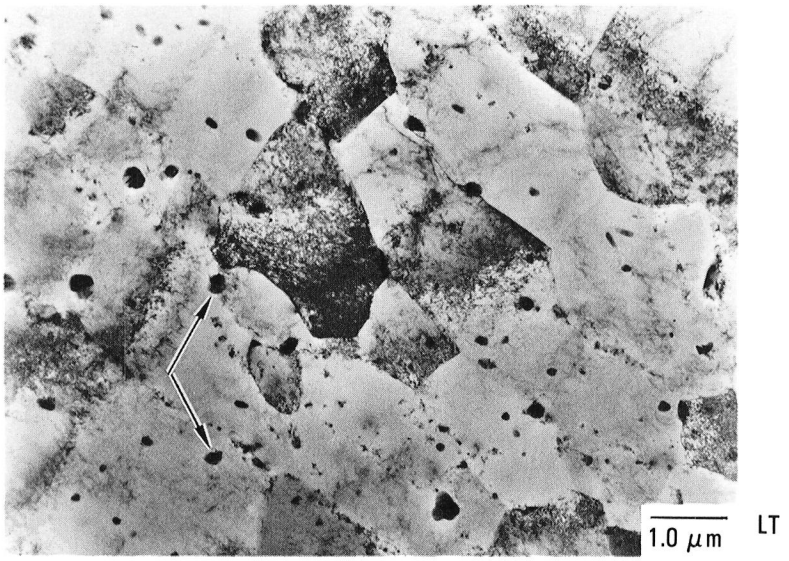

(a)

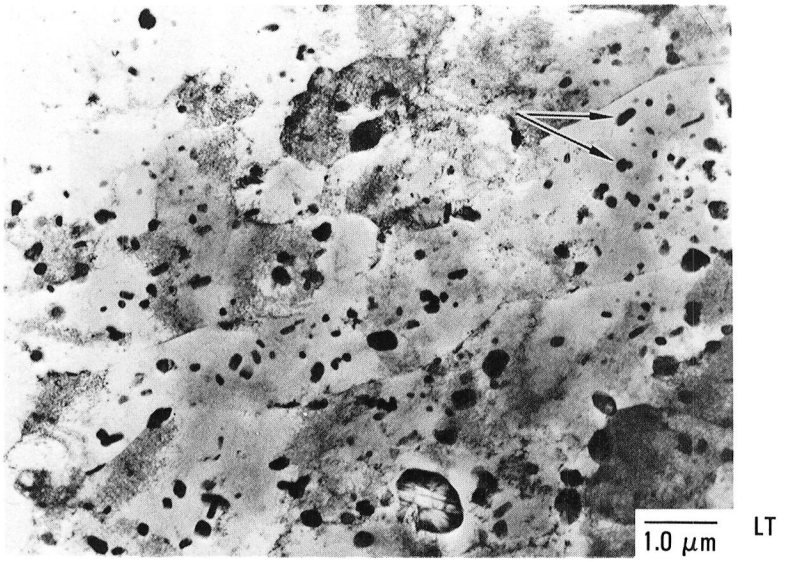

(b)

Figure 5. - Transmission electron microscopy (TEM) using bright field image of incoherent $Al_{20}Cu_2Mn_3$ dispersoid particles in P/M 2124 containing (a) 0.5 wt. pct. Mn (alloy 513709) and (b) 1.5 wt. pct. Mn (alloy 513708).

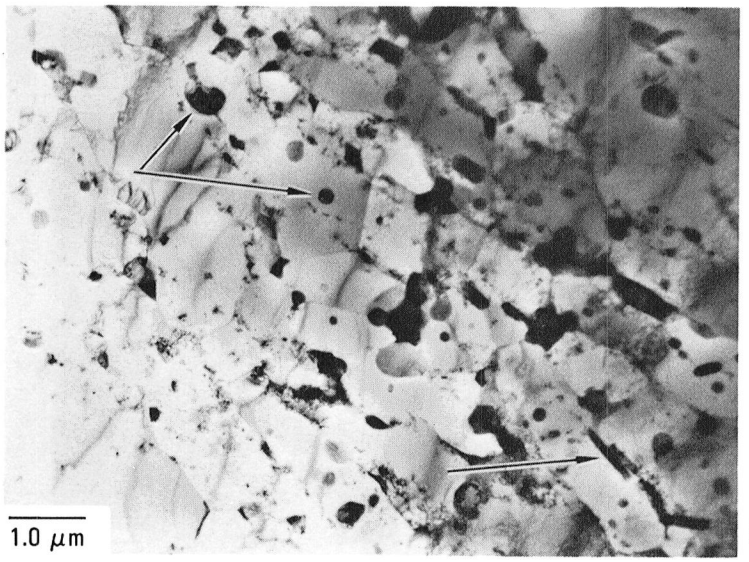

Figure 6. - Transmission electron microscopy (TEM) using bright field image of Al_9FeNi and Al_7Cu_2Fe dispersoid particles in P/M 2618 MOD Al (alloy 513707).

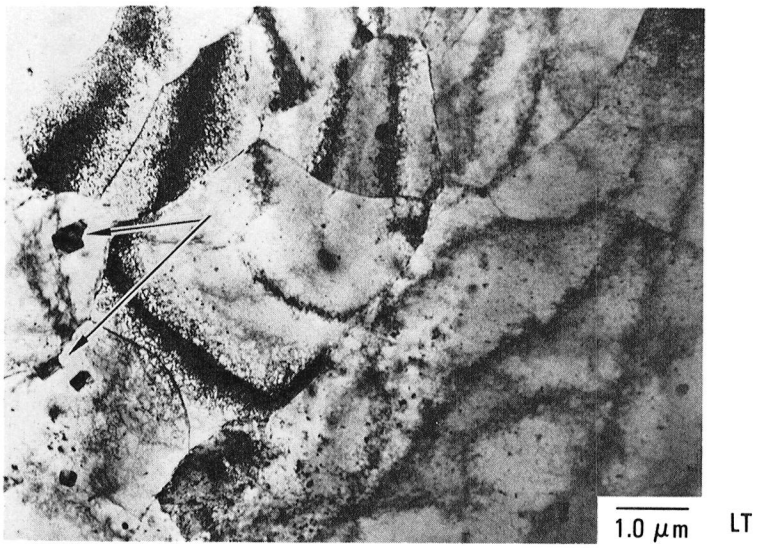

Figure 7. - Transmission electron microscopy (TEM) using bright field image of the rectangular shaped tetragonal (DO_{23}) Al_3Zr particles in alloy 514042.

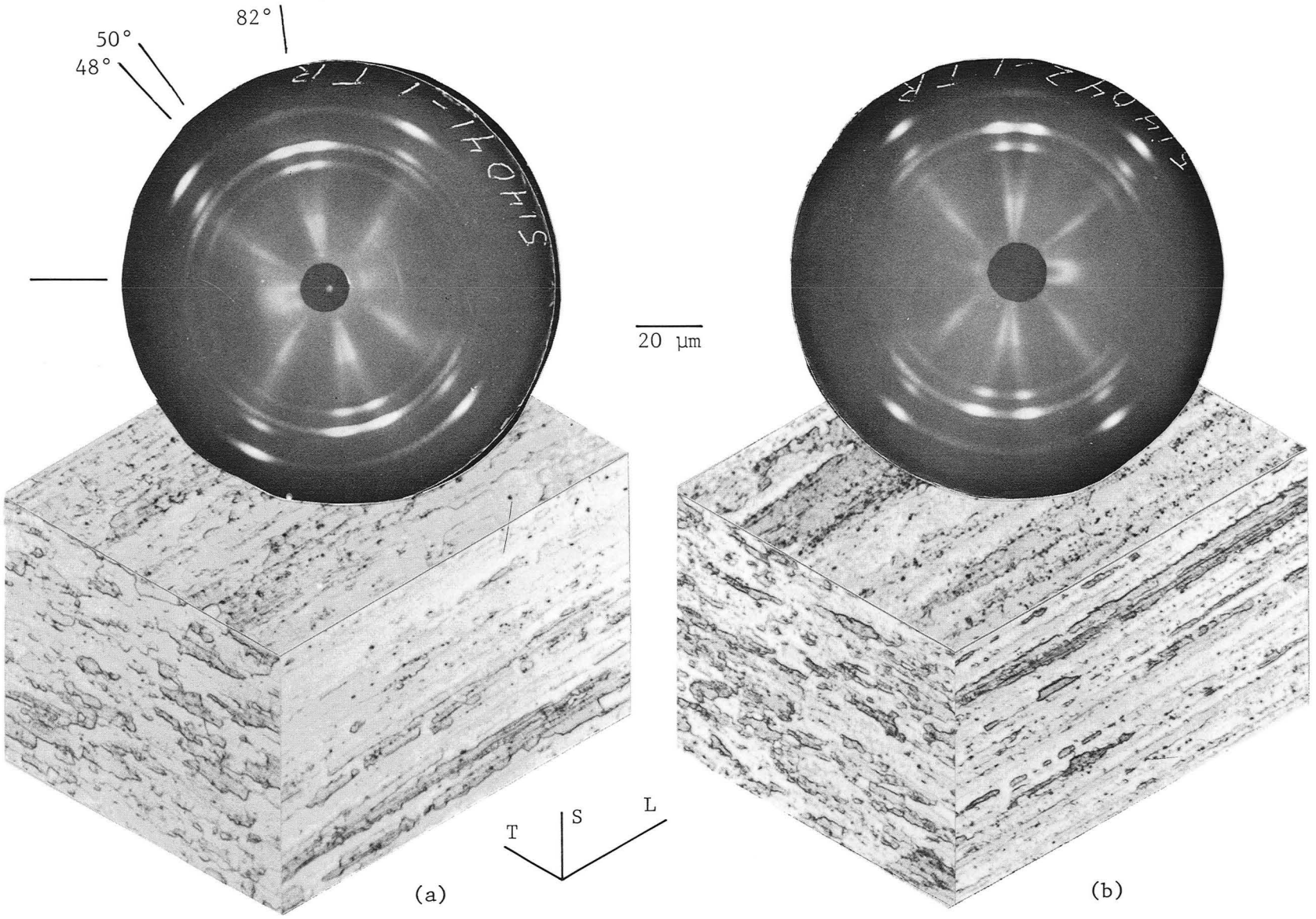

Figure 8. - Optical metallography and transmission pinhole Laue patterns showing the grain structure of P/M 2124-Zr modified alloys (a) 514041 and (b) 514042.

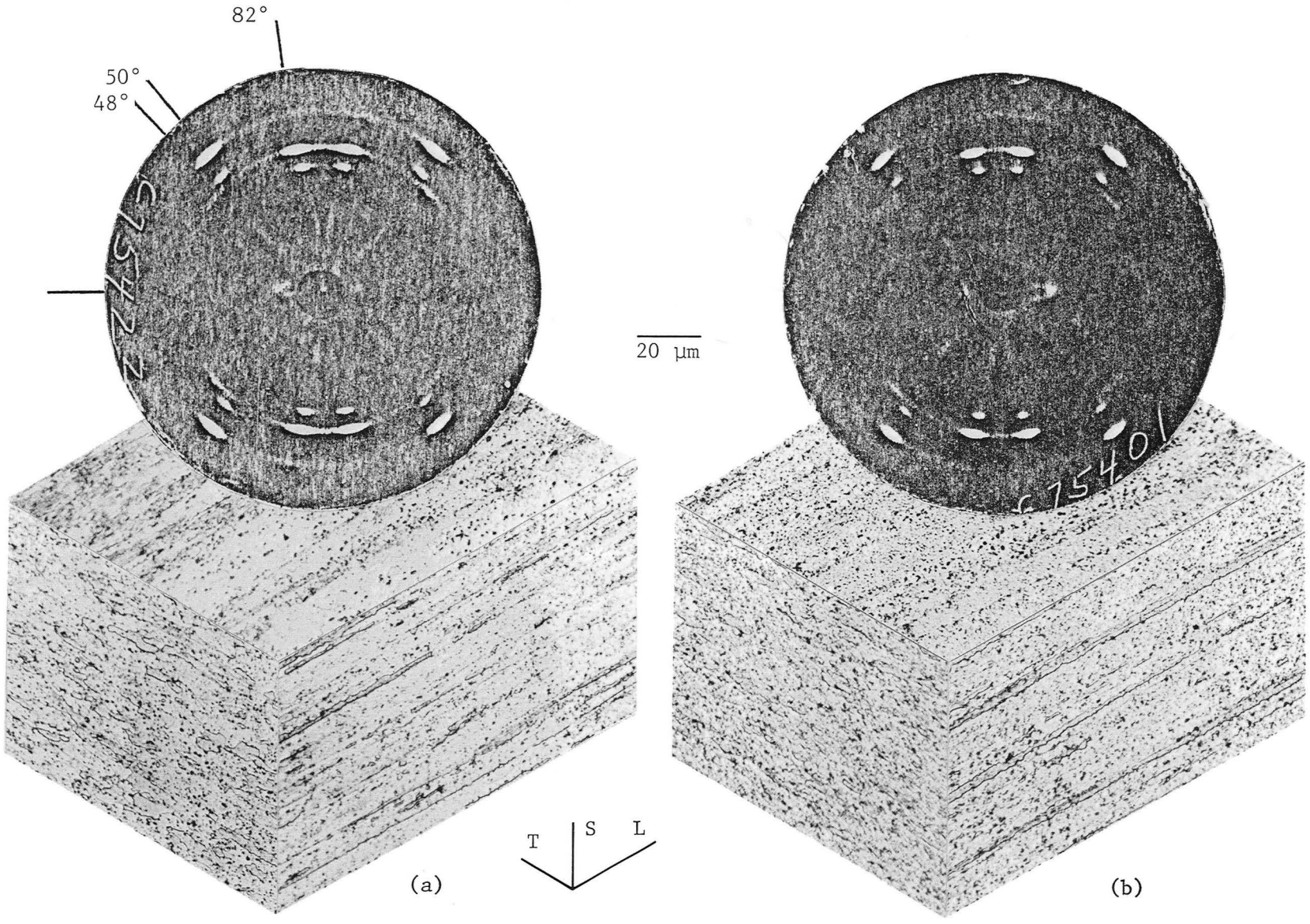

Figure 9. - Optical metallography and transmission pinhole Laue patterns showing the grain structure of alloys (a) 513709 and (b) 513708.

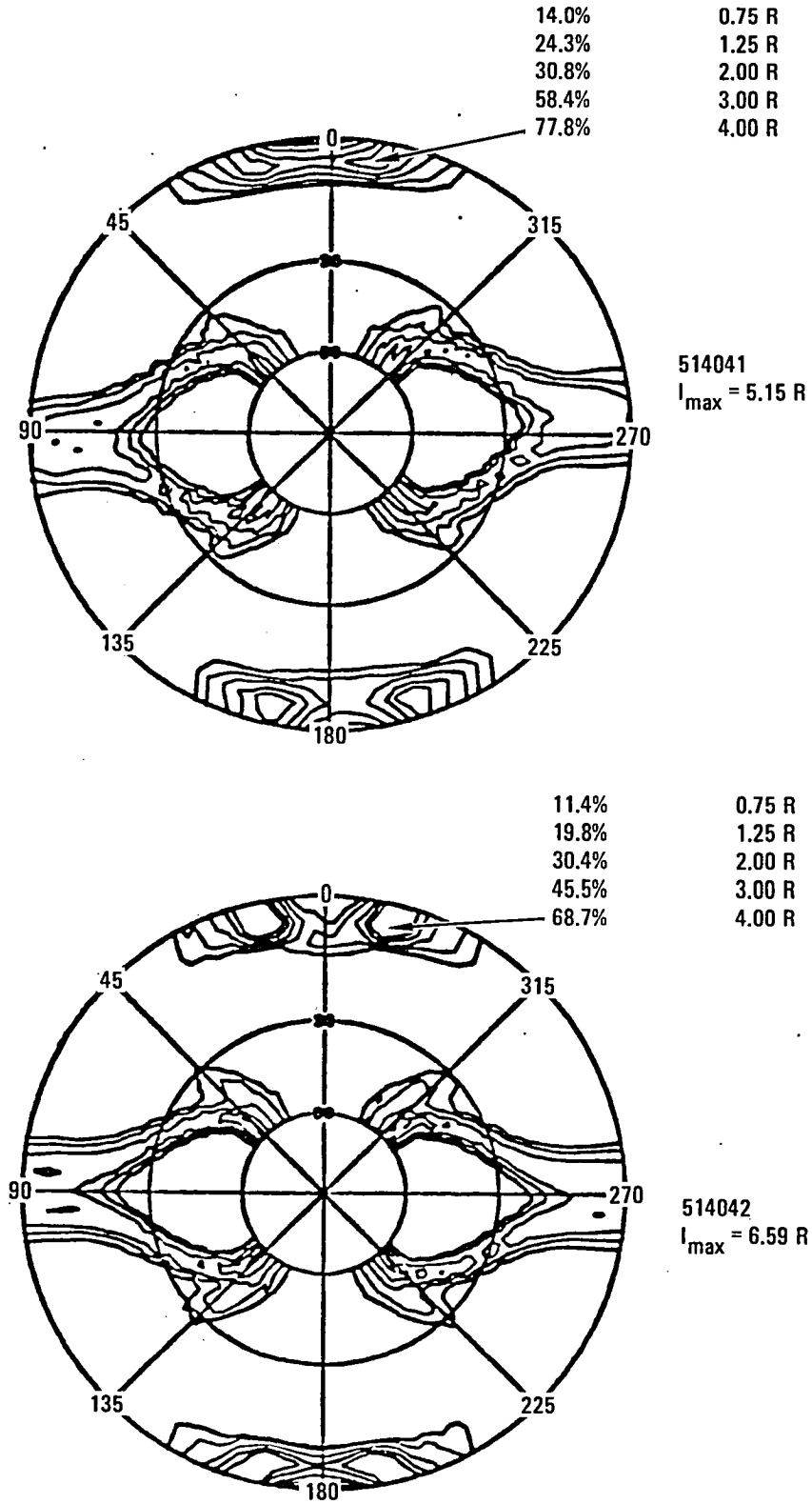

Figure 10. - The (111) pole figures showing the (110) $[1\bar{1}2]$ + (100) [001] duplex texture of P/M 2124-Zr modified Al alloys 514041 and 514042.

along the (111) diffraction ring. Since the recrystallization texture component is almost totally absent in both P/M Al alloys, the increased intensity may be a result of the more effective retardation of subgrain coalescence due to the higher volume fraction of Al_3Zr phases. The grain size and texture of wrought P/M 2XXX series Al alloys are not as sensitive to the dispersoid content and type as equivalent I/M alloys. This observation is highlighted by the grain size and texture of alloys 513888 and 513889 shown in figure 11. The addition of 1.0 wt. pct. Fe plus 1.0 wt. pct. Ni forms a fine, uniformly distributed Al_9FeNi and $Al_7Cu_2(Fe,Ni)$ phases which produce only a small decrease in grain size, texture, and degree of recrystallization relative to the Fe and Ni-free alloy.

Although no supportive metallographic evidence is provided, the role of oxides in controlling the microstructure of P/M Al alloys is probably important. During the extrusion process, the oxide network in the billet is redistributed along the extrusion direction in an extremely fine, inhomogenous manner as shown in figure 12. A distribution of particles such as these are much more effective in preventing recrystallization through the pinning of high and low angle grain boundaries than a random distribution of particles with the same volume fraction and size, Ref. 4 and 5. Consequently, the oxide distribution and fine billet grain sizes are responsible for yielding the extremely fine grain size and texture of wrought, dispersoid free, P/M Al alloys.

3.3 Mechanical Properties

The tensile properties and fracture toughness results for P/M and I/M 2124-Zr modified Al alloys and P/M 2219 MOD Al alloys are presented in the following sections for comparison with the two (2) previous NASA-LaRC research studies, Ref. 1 and 2. The currently available room and elevated temperature tensile properties after 100, 1000, and 10,000 hr exposures at 394K (250°F) and 450K (350°F) are also provided.

The presently available tensile properties and fracture toughness data (approximated by K_Q and 25 percent secant values) in the naturally aged (NA) and peak aged (PA) conditions are listed in tables 6 and 7. The behavior of the P/M 2XXX series Al alloys relative to target property goals for damage tolerance and fatigue restance (table 1) are illustrated by the histogram in figure 13. In the NA condition, only the P/M 2124-Zr modified alloy which contains 0.60 wt. pct. Zr surpasses the program strength goals, under the assumption that design minimum tensile properties are approximately 35 MPa (5 ksi) lower than typical values. In the PA condition, the P/M Al 2124 alloys (513708 and 513709) and the P/M 2219 MOD Al alloy (513887) fall short of program goals. The aging study used to determine the PA tensile properties of alloys 514041 and 514042, and I/M 503315 is not yet completed. However, based on the aging response of other P/M 2124 Al alloys, all three (3) candidates are expected to meet or exceed program strength goals. Valid fracture toughness values were not obtained in most of the alloy-temper conditions due to the reasons listed in table 7. All of the K_Q and 25 percent secant values, however, are very large and are expected to exceed program K_{IC} toughness goals of 33 Mpa $\sqrt{m}$ (30 ksi $\sqrt{in.}$).

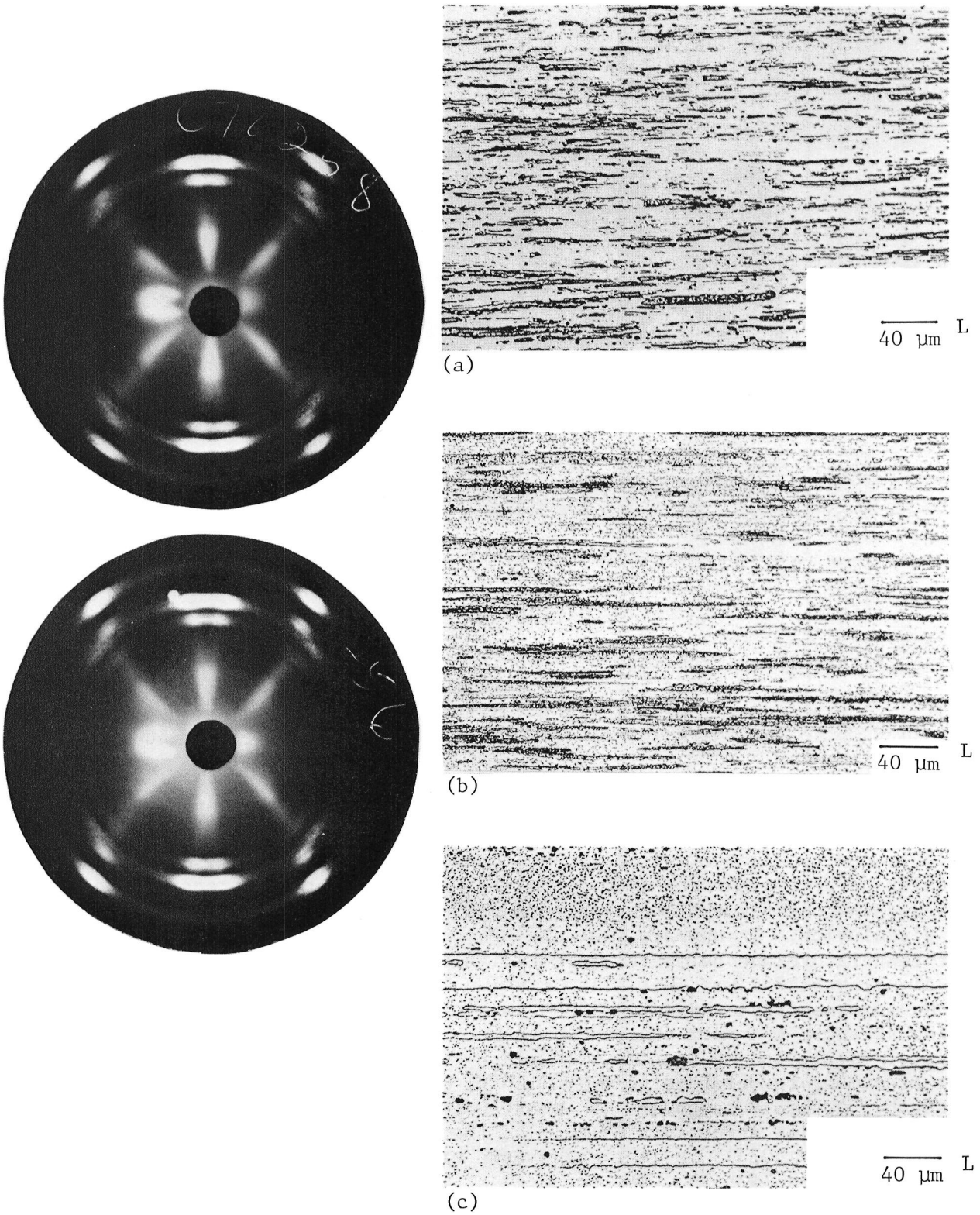

Figure 11. - Optical metallography and transmission pinhole Laue X-ray patterns showing the similarity in grain size and texture of P/M Al alloys (a) 513888 and (b) 513889, relative to (c) I/M Al alloy 503315.

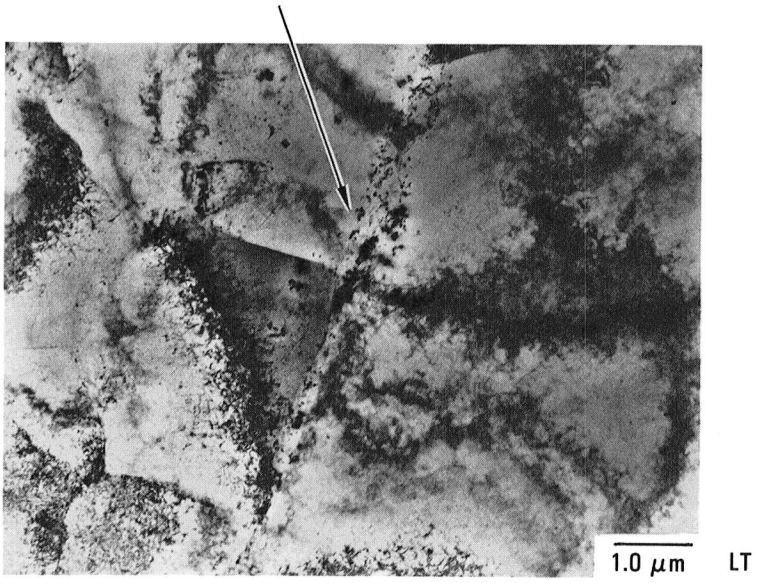

Figure 12. - Transmission electron microscopy (TEM) using bright field image of inhomogeneously distributed oxides along a grain boundary elongated in the extrusion direction in P/M 2124-Zr modified Al alloy 514041.

The improved combination of strength and fracture toughness in P/M 2124-Zr modified alloys 514041 and 514042 relative to P/M Al 2124 is achieved by increasing the solution heat treatment temperature from 766K (920°F) to 775K (935°F), and replacement of $Al_{20}Cu_2Mn_3$ dispersoids with Al_3Zr. An increase in solution heat treatment temperature is known to improve strength levels provided that sufficient undissolved soluble Al_2CuMg and Al_2Cu is available for dissolution. It appears that the previously selected solution heat treatment temperature was below the eutectic as observed in figure 14. For example, P/M Al alloy 513887 was initially solution heat treated at 777K (940°F). A low Cu supersaturation and many coarse, undissolved Al_2Cu particles resulted in low strength and poor fracture toughness values. It is predicted on the basis of figure 15 and results obtained by Lockheed that an increase in solution heat treatment temperature to 802K (985°F) would significantly increase the strength. Fracture toughness is observed to be commensurate with other P/M Al alloys of similar strength. Similarly, the strength of P/M Al alloys 514041, 514042, and I/M 503315 is improved by the higher supersaturation of Cu and Mg achieved at 775K (935°F). The presence of incoherent $Al_{20}Cu_2Mn_3$, coarse Al_2CuMg and coarse grain structures in I/M 503315, apparently combine to degrade toughness levels by approximately 10 percent relative to alloys 514041 and 514042.

TABLE 6. - TENSILE PROPERTIES OF P/M 2XXX AL ALLOY EXTRUSIONS

Sample No.	Temper (10)	Yield Strength MPa	Yield Strength (ksi)	Tensile Strength MPa	Tensile Strength (ksi)	El. (%)	R.A. (%)
PM 2618	NA	384	(55.7)	484	(70.2)	12.0	--
	PA (1)	407	(59.0)	455	(66.0)	10.0	--
PM 2124 - High Mn	NA	420	(60.9)	520	(75.4)	10.0	--
	PA (2)	453	(65.7)	494	(71.7)	12.0	--
PM 2124 - Low Mn	NA	419	(60.8)	518	(75.1)	16.0	--
	PA (2)	451	(65.4)	497	(72.0)	12.0	--
PM 2219	NA	383	(55.4)	498	(72.3)	14.5	14.5
	PA (3)	436	(63.2)	514	(74.5)	13.7	33.3
PM 2618 - Mod A	NA	360	(52.2)	470	(68.1)	16.0	13.2
	PA (4)	364	(52.8)	420	(60.9)	13.0	41.5
PM 2618 - Mod B	NA	388	(56.2)	506	(73.3)	16.0	15.2
	PA (5)	418	(60.6)	471	(68.3)	12.7	28.0
PM 2124 - Low Zr	NA	438	(63.5)	536	(77.6)	17.5	19.5
	PA (5)	493	(71.4)	532	(77.2)	14.0	31.0
PM 2124 - High Zr	NA	463	(67.2)	571	(82.8)	15.0	19.0
	PA (5)	509	(73.8)	548	(79.5)	11.0	27.0
IM 2034	NA	442	(64.1)	572	(82.8)	14.0	13.0
	PA (5)	529	(76.8)	575	(83.4)	11.0	28.0

Notes:
(1) Aged 12 hours at 464 K (375°F).
(2) Aged 4 hours at 464 K (375°F).
(3) Aged 4 hours at 450 K (350°F).
(4) Aged 8 hours at 464 K (375°F).
(5) Aged 4 hours at 464 K (375°F).
(6) Solution heat treated at 766 K (920°F).
(7) Solution heat treated at 772 K (940°F).
(8) Solution heat treated at 802 K (985°F).
(9) Solution heat treated at 775 K (935°F).
(10) Stretched 1.5 - 2.0%.

TABLE 7. - FRACTURE TOUGHNESS OF P/M 2XXX AL ALLOY EXTRUSIONS

Sample No.	Temper (7)	Yield Strength		K_Q		25% Secant Value	
		MPa	(ksi)	MPa$\sqrt{m}$	(ksi$\sqrt{in.}$)	MPa$\sqrt{m}$	(ksi$\sqrt{in.}$)
PM 2618	NA	384	(55.7)	42.2	(38.4) (1,3)	71.3	(64.9)
	PA (4)	407	(59.0)	41.0	(37.3) (1,3)	55.7	(50.7)
PM 2124 - High Mn	NA	420	(60.9)	44.6	(40.6) (1,3,4)	78.8	(71.7)
	PA (4)	410	(60.3)	53.0	(48.2) (1,2,3,)	72.3	(65.8)
PM 2124 - Low Mn	NA	419	(60.8)	55.7	(50.7) (1,2,3)	100.2	(91.2)
	PA (4)	405	(58.7)	53.3	(48.5) (1,2,3)	91.9	(83.6)
PM 2219	NA	383	(55.4)	40.7	(37.1) (1,3)	81.4	(74.0)
	PA (5)	436	(63.2)	59.1	(53.8) (1,2,3)	93.1	(84.8)
PM 2618 - Mod A	NA	403	(58.5)	45.8	(41.6) (1,3)	88.6	(80.6)
	PA (6)	414	(60.0)	55.1	(50.1) (1,2,3)	95.6	(87.0)
PM 2618 - Mod B	NA	425	(61.6)	45.0	(40.6) (1,3)	67.4	(61.3)
	PA (6)	421	(61.1)	38.1	(34.7) (1,3)	54.2	(49.3)
PM 2124 - Low Zr	NA	438	(63.5)	53.9	(49.0) (1,2,3)	100.1	(91.0)
	PA (8)	493	(71.4)	--	(58.0)	--	(98.6)
PM 2124 - High Zr	NA	463	(67.2)	53.8	(49.0) (1,2,3,4)	95.2	(86.6)
	PA (8)	509	(73.8)	--	(52.7)	--	(77.0)
IM 2034	NA	442	(64.1)	48.7	(44.3) (1,3,4)	93.1	(84.8)
	PA (8)	529	(76.8)	--	(31.6)	--	(43.3)

Notes:
(1) Invalid due to insufficient specimen thickness.
(2) Invalid due to insufficient fatigue precrack length.
(3) Invalid due to $P_{max}/P_o > 1.10$.
(4) Aged 12 hours at 464 K (375°F).
(5) Aged 4 hours at 450 K (350°F).
(6) Aged 16 hours at 450 K (350°F).
(7) Stretched 1.5 - 2.0%.
(8) Aged 4 hours at 464K (375°F).

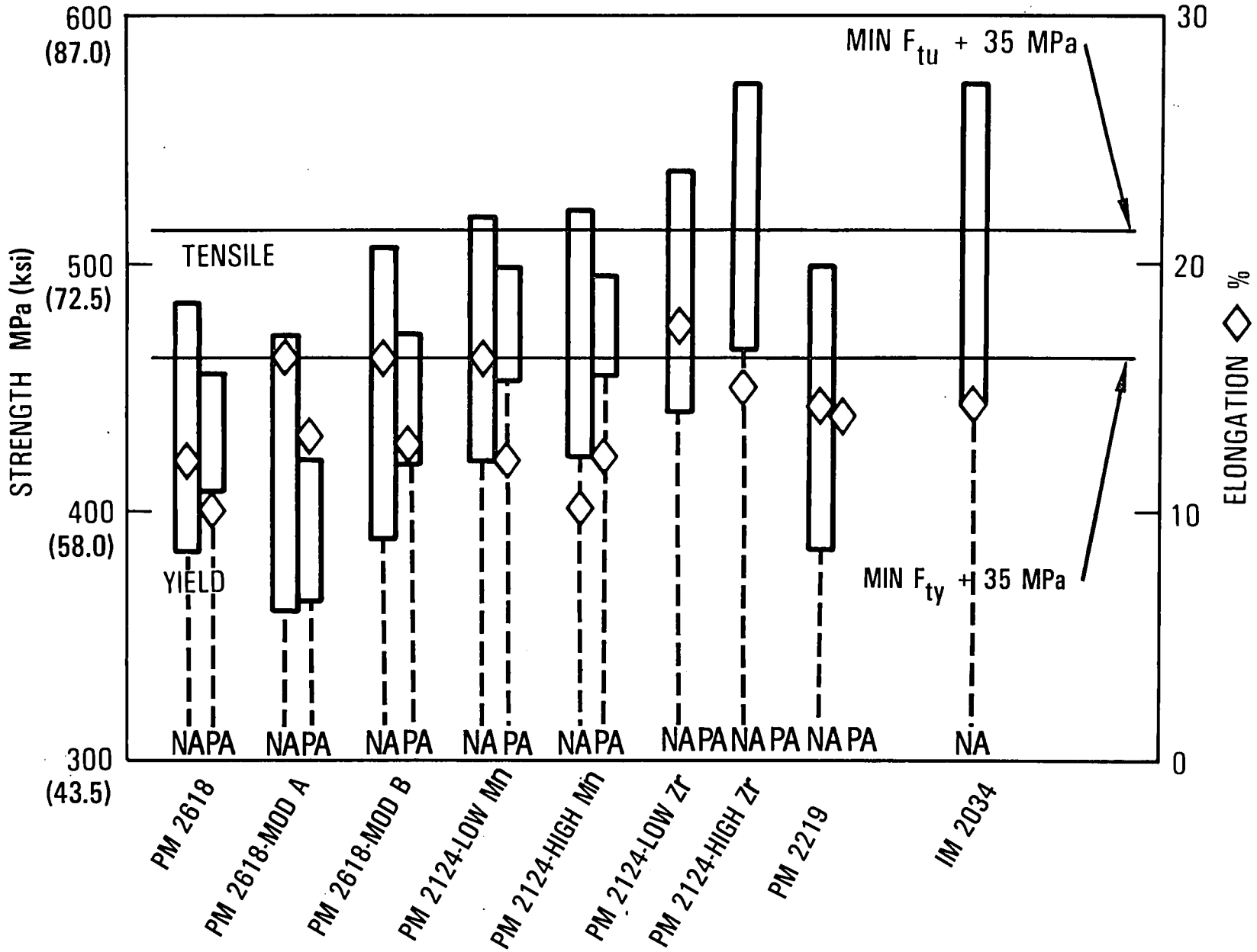

Figure 13. - Histograms showing the performance of NASA LaRC P/M 2XXX Al alloys relative to the strength requirements for damage tolerance and fatigue resistance; F_{tu} = 479 MPa (68 ksi) and F_{ty} = 427 MPa (62 ksi).

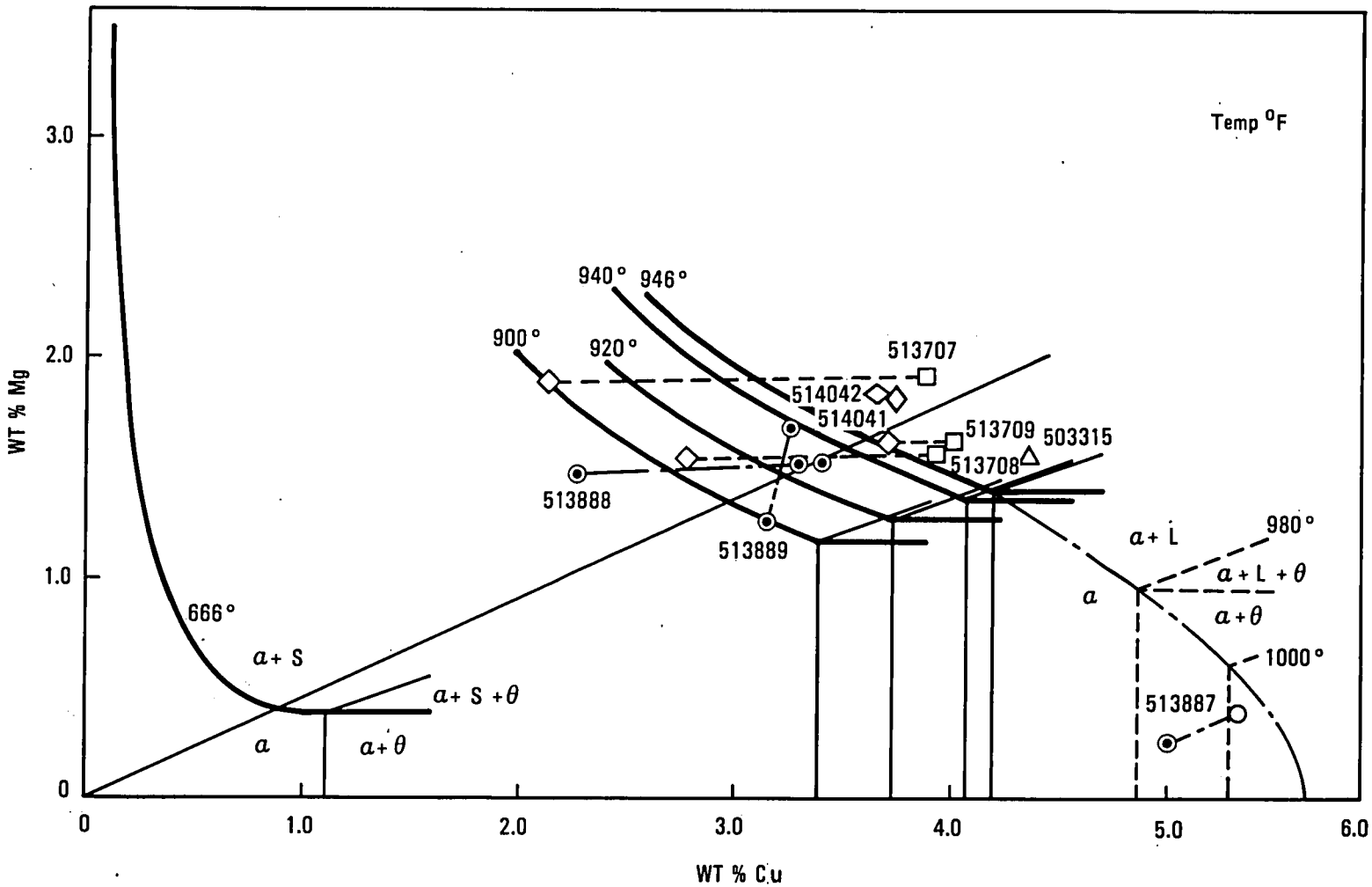

Figure 14. - The Al-Cu-Mg ternary solvus diagram.

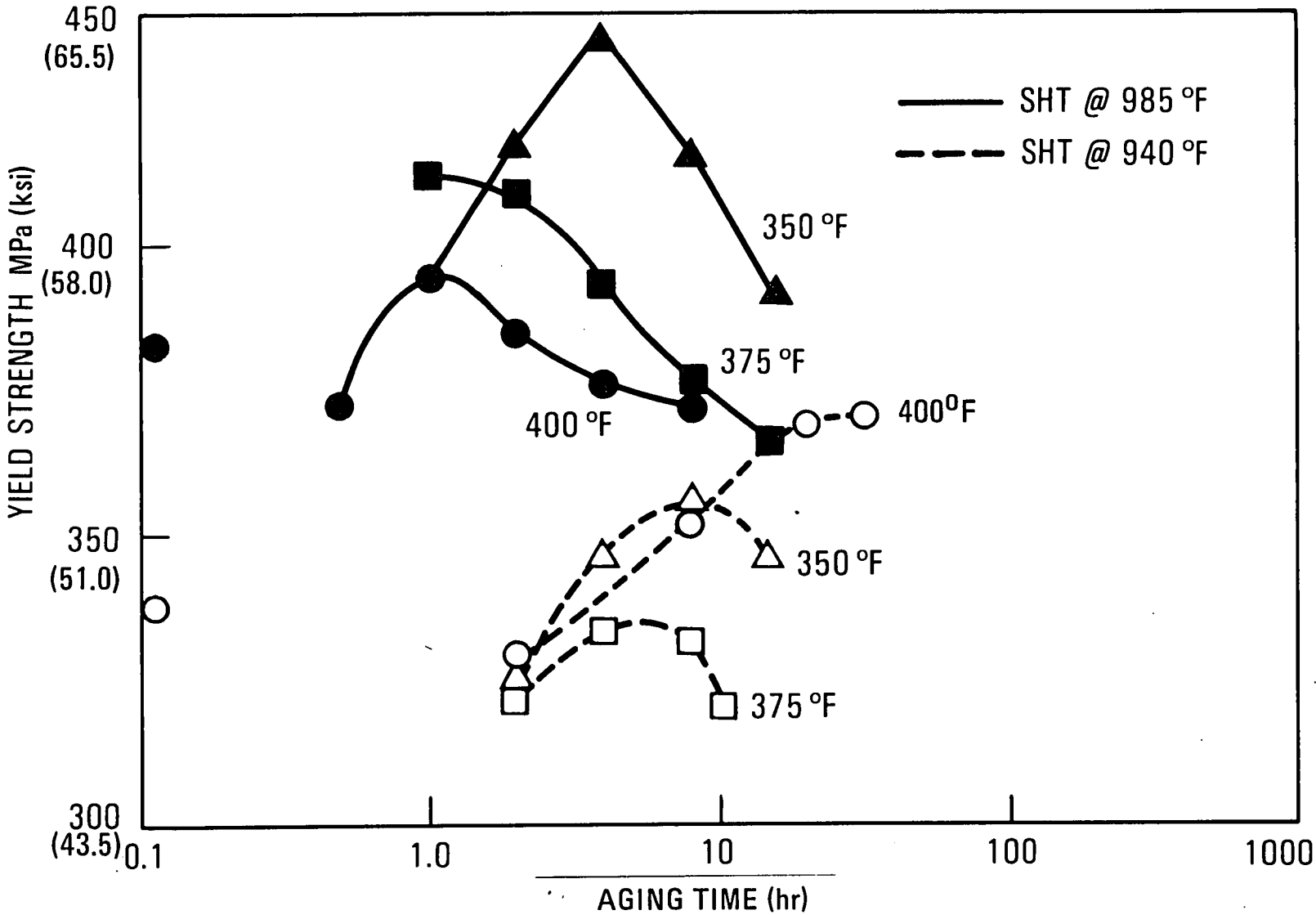

Figure 15. - The aging response of P/M 2219 Al alloy (513887) solution heat treated at 777K (940°F) and 802K (985°F).

In the NA condition, an increase in the Zr content from 0.12 wt. pct. in alloy 514041 to 0.60 wt. pct. in alloy 514042 results in an improvement in strength of 25 MPa (3.6 ksi), with a reduction of 25 percent secant toughness values of only 4.9 MPa $\sqrt{m}$ (4.4 ksi $\sqrt{in.}$). For the P/M 2124 Al alloy, an increase in the Mn content from 0.5 wt. pct. in alloy 513709 to 1.5 wt. pct. in alloy 513708 is observed to improve strength slightly and reduce the 25 percent secant toughness value by 19.5 MPa $\sqrt{m}$ (17.8 ksi $\sqrt{in.}$). Scanning electron microscopy (SEM) fractography shows a correlation between Mn content and the size and distribution of dimples, as observed in figure 16. These microstructural observations suggest that the $Al_{20}Cu_2Mn_3$ dispersoids shown in figure 5 actively participate in void formation. An increase in the Mn content reduces the interparticle spacing, thereby promoting earlier void coalescence and lower fracture toughness. Although SEM fractography of the P/M 2124-Zr modified Al alloys is not available, the insensitivity of K_Q to the Zr content suggests that Al_3Zr may not be as harmful to toughness as $Al_{20}Cu_2Mn_3$ dispersoids. The relative difference between matrix-particle interfacial strengths of coherent and incoherent phases may be an important metallurgical parameter, as described in the literature, Ref. 6.

The strengthening of P/M 2XXX Al alloys with coherent Al_3Zr phases may be associated with either the inhibition of dislocation motion during slip by the particles or the retardation of recovery and recrystallization mechanisms as shown by the sharper crystallographic texture. It has been suggested in alloy development studies on P/M Al-Li alloy systems that both mechanisms are important in accounting for the strengthening behavior. In a chill cast 7XXX Al alloy containing 1.0 wt. pct. Zr, the optimum hardness level is sensitive to the preheat temperature, and consequently the size and distribution of coherent Al_3Zr, Ref. 7. Since the solution heat treat and preheat temperatures used for 2XXX and 7XXX Al alloys are appropriate for aging Al_3Zr, samples of the P/M 2124-Zr modified alloys in the -F temper extrusions were isothermally soaked in a salt bath at 774K (935°F) in order to determine the aging response. Although the results presented in figure 17 were ambiguous, several interesting observations were made. An increase in the Zr content from 0.12 wt. pct. to 0.60 wt. pct. in the -F temper yielded an R_B hardness increase of nearly 250 percent from 9.3 to 32.3. During solution heat treatment, the hardness of both alloys increases to a maximum after soaking times of approximately 30 minutes. In this optimum condition, the difference in hardness values between the alloys is reduced significantly, probably due to the influence of a high volume fraction of fine GPB zones. Gradual softening ensues as a function of soaking time after the 30 minutes peak condition. Metallographic observation of specimens heated before and after the peak are necessary to isolate the changes in microstructure that contribute to this behavior. Soaking times between 0 and 15 minutes are also needed to determine if a dissolution peak exists at shorter times.

The currently available room and elevated temperature tensile properties after 100, 1000, and 10,000 hours exposure at 394K (250°F) and 450K (350°F) are provided in tables 8 - 11. Results from the alloys given 5 to 6 percent cold work prior to artificial aging are used to show the effect of dispersoid content and exposure time, in figures 18-21. The room and elevated temperature tensile properties of P/M 2XXX Al alloys are insensitive to the volume

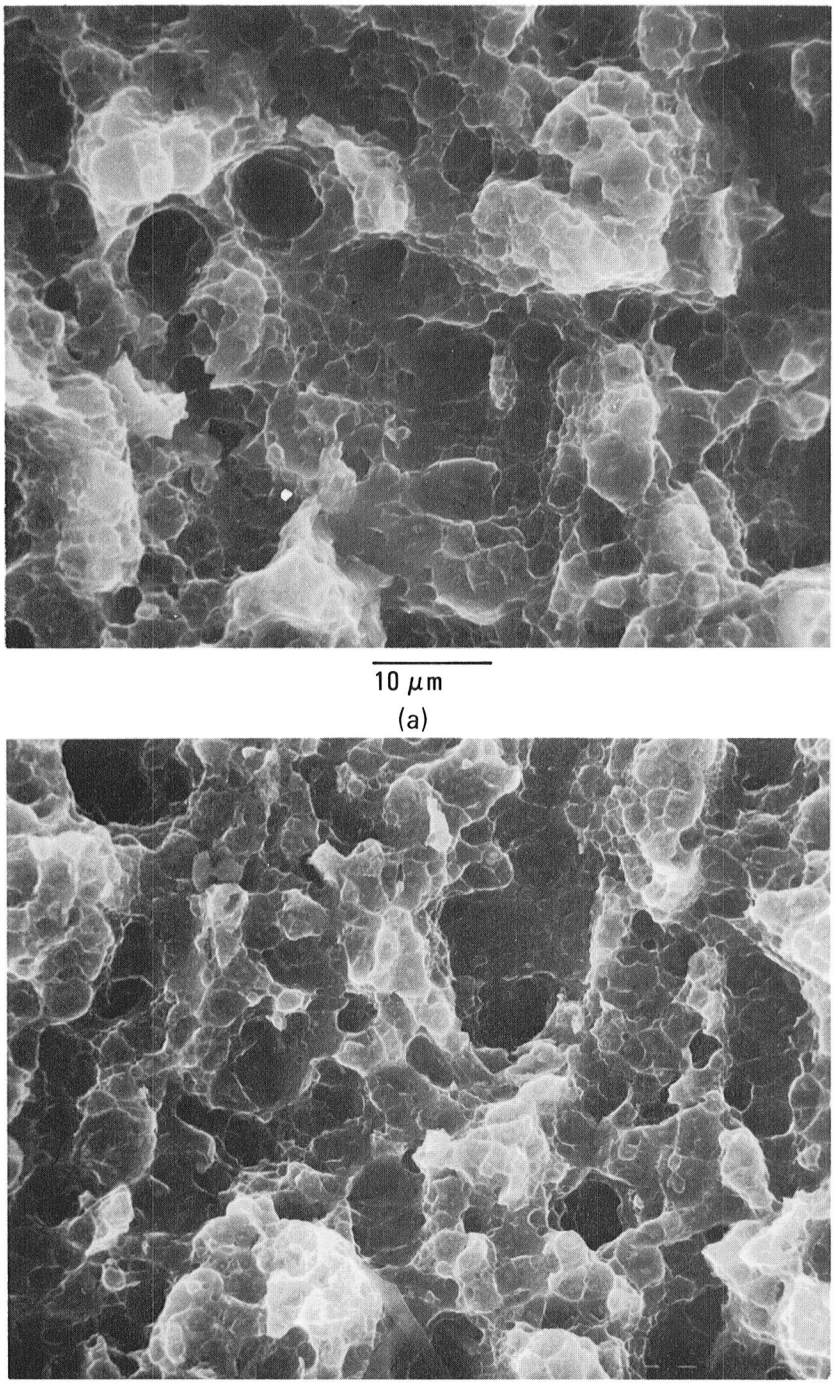

Figure 16. - Scanning electron microscopy (SEM) fractography showing the decrease in dimple size and spacing when the Mn content is increased from (a) 0.5 wt. pct. in alloy 513709 to (b) 1.5 wt. pct. in alloy 513708.

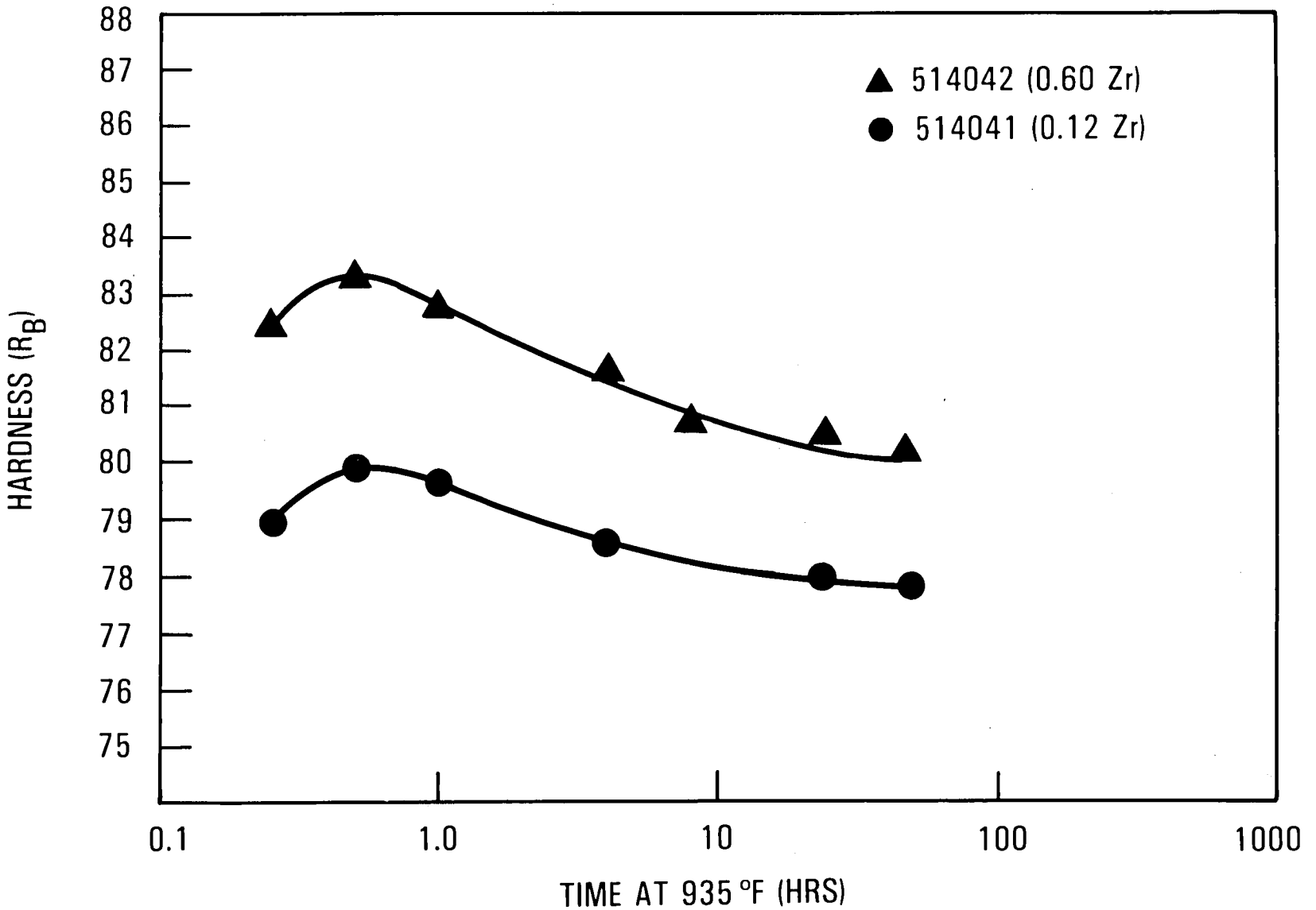

Figure 17. - Isothermal aging curves for P/M 2124-Zr modified alloys 514041 and 514042 soaked at 774 K (935°F).

TABLE 8. - ROOM TEMPERATURE TENSILE PROPERTIES OF P/M 2XXX AL ALLOYS AFTER EXPOSURE TO 394K (250°F)

Sample No.	Temper	Exposure Time (Hours)	Yield Strength		Tensile Strength		El. (%)	R.A. (%)
			MPa	(ksi)	MPa	(ksi)		
513707	A	100	370	(53.7)	437	(63.4)	9	22
		1,000	373	(54.1)	440	(63.9)	10	22
		10,000	387	(56.2)	450	(65.3)	10	20
	B	100	381	(55.3)	441	(64.0)	8	22
		1,000	382	(55.4)	440	(63.8)	10	26
		10,000	439	(63.8)	485	(70.3)	8	20
513708	C	100	414	(60.0)	471	(68.3)	12	34
		1,000	421	(61.1)	481	(69.8)	13	38
		10,000	392	(56.9)	466	(67.6)	12	33
	D	100	553	(80.2)	520	(75.4)	9	18
		1,000	570	(82.7)	548	(79.5)	11	29
		10,000	425	(61.6)	487	(70.6)	11	32
513709	C	100	409	(59.3)	467	(67.7)	11	34
		1,000	414	(60.1)	473	(68.7)	15	42
		10,000	389	(56.4)	461	(66.9)	14	41
	D	100	527	(76.4)	559	(79.8)	11	28
		1,000	510	(73.9)	537	(77.7)	12	32
		10,000	423	(61.4)	487	(70.6)	13	38
513888	E	100	450	(65.3)	476	(69.0)	12	35
		1,000	446	(64.6)	476	(69.0)	12	43
513889	E	100	468	(67.8)	497	(72.1)	12	32
		1,000	462	(67.0)	495	(71.7)	12	30

Notes:
(A) Stretched 1.5 - 2.0%, Aged 19 hours at 472K (390°F).
(B) Cold Rolled 5.0%, Aged 6 hours at 464K (375°F).
(C) Stretched 1.5 - 2.0%, Aged 12 hours at 464K (375°F).
(D) Cold Rolled 5.0%, Aged 3 hours at 464K (375°F).
(E) Stretched 6.0%, Aged 16 hours at 450K (350°F).

TABLE 9. - ELEVATED TEMPERATURE TENSILE PROPERTIES OF P/M 2XXX AL ALLOYS AT 394K (250°F)

Sample No.	Temper	Exposure Time (Hours)	Yield Strength		Tensile Strength		El. (%)	R.A. (%)
			MPa	(ksi)	MPa	(ksi)		
513707	A	100	332	(48.3)	386	(56.0)	13.0	31.4
		1,000	326	(47.3)	373	(54.1)	14.0	36.0
		10,000	353	(51.1)	392	(56.8)	14.0	32.7
	B	100	342	(49.6)	381	(55.2)	13.8	31.8
		1,000	347	(50.4)	386	(56.0)	11.0	28.0
		10,000	390	(56.6)	413	(59.8)	14.5	32.8
513708	C	100	371	(53.9)	416	(60.4)	17.0	45.6
		1,000	360	(52.2)	405	(58.7)	17.0	46.0
		10,000	341	(49.5)	390	(56.6)	16.5	41.6
	D	100	452	(65.6)	521	(75.6)	11.8	16.8
		1,000	436	(63.3)	461	(66.9)	14.0	40.0
		10,000	368	(53.3)	405	(58.7)	16.5	47.8
513709	C	100	362	(52.2)	409	(59.3)	20.5	55.7
		1,000	348	(50.5)	387	(56.1)	19.0	57.0
		10,000	341	(49.3)	384	(55.7)	18.5	54.4
	D	100	454	(65.9)	514	(74.6)	12.2	18.6
		1,000	446	(64.7)	467	(67.7)	17.5	50.0
		10,000	376	(54.6)	415	(60.1)	20.0	50.9
513888	E	100	421	(61.0)	434	(62.9)	17.0	48.8
		1,000	413	(59.8)	426	(61.8)	17.0	50.7
513889	E	100	427	(61.9)	441	(63.9)	18.0	46.5
		1,000	413	(59.8)	427	(61.8)	17.5	50.7

Notes:
(A) Stretched 1.5 - 2.0%, Aged 19 hours at 472 K (390°F).
(B) Cold Rolled 5.0%, Aged 6 hours at 464 K (375°F).
(C) Stretched 1.5 - 2.0%, Aged 12 hours at 464 K (375°F).
(D) Cold Rolled 5.0%, Aged 3 hours at 464 K (375°F).
(E) Stretched 6.0%, Aged 16 hours at 450 K (350°F).

TABLE 10. - ROOM TEMPERATURE TENSILE PROPERTIES OF P/M 2XXX AL ALLOYS AFTER EXPOSURE TO 450K (350°F)

Sample No.	Temper	Exposure Time (Hours)	Yield Strength		Tensile Strength		El. (%)	R.A. (%)
			MPa	(ksi)	MPa	(ksi)		
513707	A	100	353	(51.2)	426	(61.8)	10	23
		1,000	308	(44.6)	397	(57.6)	11	23
		10,000	196	(28.4)	307	(44.5)	13	24
	B	100	366	(53.1)	431	(62.5)	9	21
		1,000	314	(45.6)	391	(56.8)	10	21
		10,000	213	(30.9)	307	(44.5)	13	37
513708	C	100	370	(53.7)	444	(64.4)	13	37
		1,000	280	(40.6)	380	(55.1)	15	38
		10,000	164	(24.9)	275	(39.8)	19	34
	D	100	402	(58.2)	468	(67.9)	12	31
		1,000	299	(43.4)	385	(55.7)	12	26
		10,000	176	(25.5)	276	(40.0)	18	34
513709	C	100	372	(54.0)	442	(64.1)	14	42
		1,000	291	(42.3)	383	(55.5)	15	40
		10,000	165	(23.9)	270	(39.2)	20	42
	D	100	406	(58.9)	468	(67.9)	13	44
		1,000	305	(44.2)	388	(56.2)	16	46
		10,000	176	(25.5)	275	(39.9)	18	38
513888	E	100	360	(52.1)	421	(61.0)	15	38
		1,000	265	(38.4)	340	(49.3)	15	41
513889	E	100	344	(49.9)	414	(60.0)	14	43
		1,000	251	(36.3)	336	(48.7)	17	46

Notes:
(A) Stretched 1.5 - 2.0%, Aged 19 hours at 472K (390°F).
(B) Cold Rolled 5.0%, Aged 6 hours at 464K (375°F).
(C) Stretched 1.5 - 2.0%, Aged 12 hours at 464K (375°F).
(D) Cold Rolled 5.0%, Aged 3 hours at 464K (375°F).
(E) Stretched 6.0%, Aged 16 hours at 450K (350°F).

TABLE 11. - ELEVATED TEMPERATURE TENSILE PROPERTIES OF P/M 2XXX AL ALLOYS AT 450K (350°F)

Sample No.	Temper	Exposure Time (Hours)	Yield Strength MPa	Yield Strength (ksi)	Tensile Strength MPa	Tensile Strength (ksi)	El. (%)	R.A. (%)
513707	A	100	279	(40.4)	299	(43.4)	26.8	54.6
		1,000	248	(36.0)	273	(39.6)	26.0	60.0
		10,000	185	(26.8)	201	(29.1)	33.0	65.5
	B	100	270	(39.2)	299	(43.4)	28.0	53.1
		1,000	246	(35.7)	274	(39.7)	26.0	58.0
		10,000	193	(27.9)	225	(32.6)	27.5	62.4
513708	C	100	270	(39.1)	301	(43.7)	26.5	63.7
		1,000	214	(31.1)	252	(36.6)	26.0	67.8
		10,000	142	(20.5)	181	(26.3)	33.5	74.7
	D	100	287	(41.7)	313	(48.4)	24.2	64.0
		1,000	221	(32.0)	263	(36.1)	27.0	70.0
		10,000	153	(22.1)	187	(27.1)	33.5	75.9
513709	C	100	272	(39.4)	309	(44.9)	26.2	70.0
		1,000	223	(32.4)	253	(36.7)	26.0	77.0
		10,000	142	(20.5)	179	(25.9)	33.5	80.4
	D	100	285	(41.4)	317	(46.0)	25.5	70.6
		1,000	240	(34.8)	267	(38.7)	26.0	74.0
		10,000	158	(22.9)	190	(27.5)	31.0	79.2
513888	E	100	241	(34.9)	262	(38.0)	27.0	75.6
		1,000	244	(35.3)	256	(37.1)	24.5	73.8
513889	E	100	266	(38.5)	279	(40.4)	20.5	70.1
		1,000	200	(29.0)	221	(32.1)	27.5	78.0

Notes:
(A) Stretched 1.5 - 2.0%, Aged 19 hours at 472K (390°F).
(B) Cold Rolled 5.0%, Aged 6 hours at 464K (375°F).
(C) Stretched 1.5 - 2.0%, Aged 12 hours at 464K (375°F).
(D) Cold Rolled 5.0%, Aged 3 hours at 464K (375°F).
(E) Stretched 6.0%, Aged 16 hours at 450K (350°F).

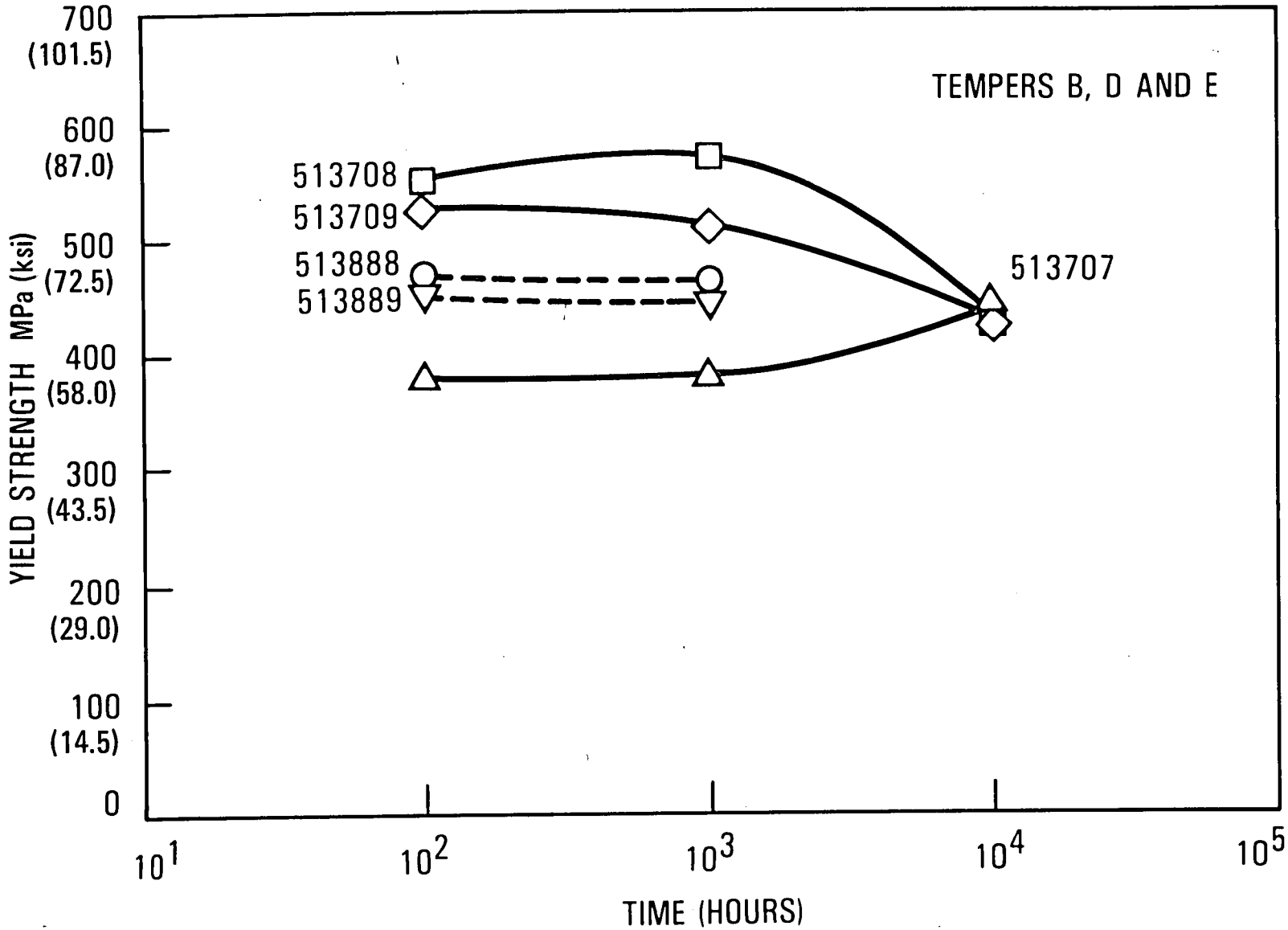

Figure 18. - Room temperature strength of P/M 2XXX Al alloys after exposure at 394 K (250°F).

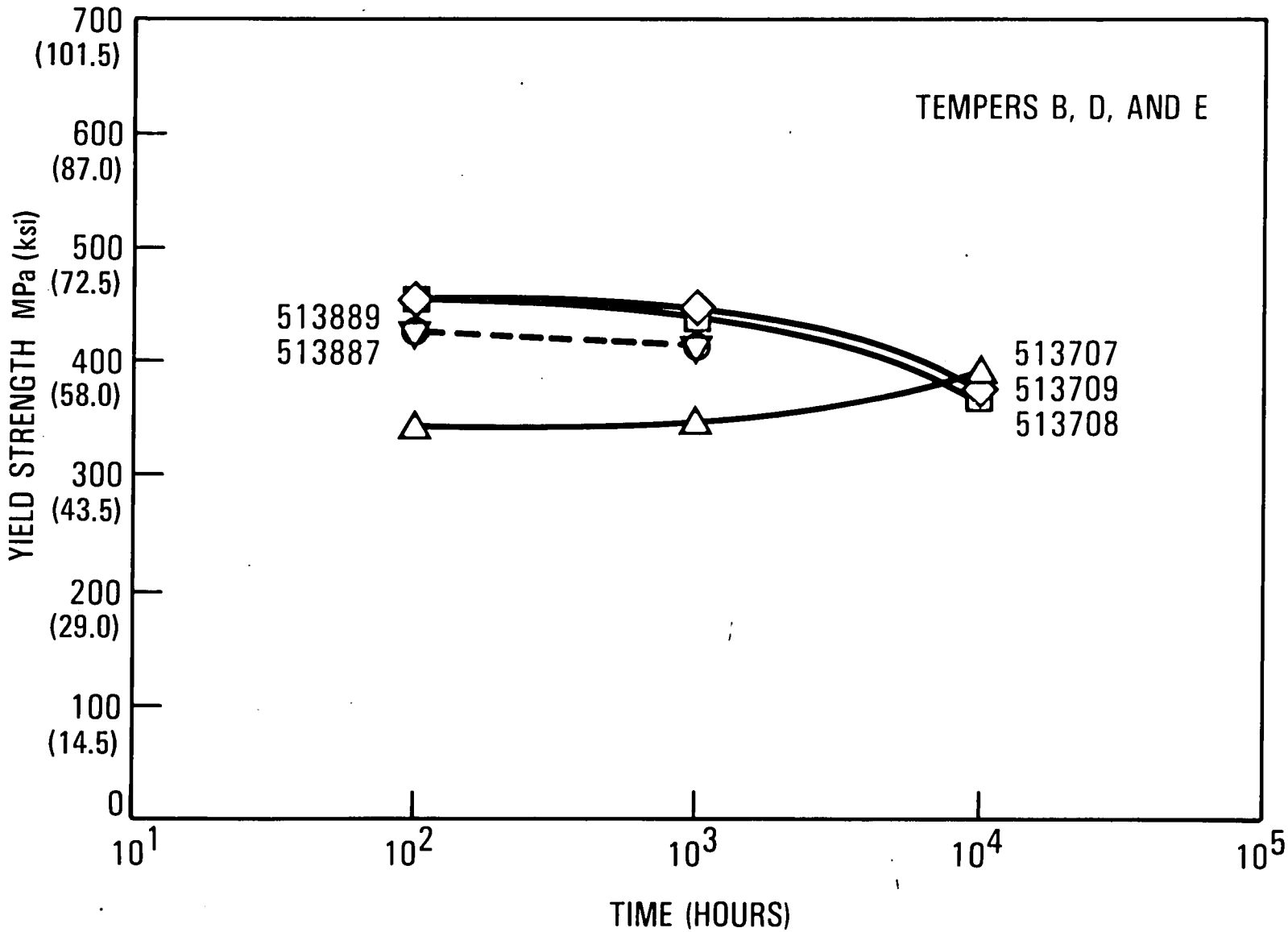

Figure 19. - Elevated temperature strength of P/M 2XXX Al alloys after exposure at 394 K (250°F).

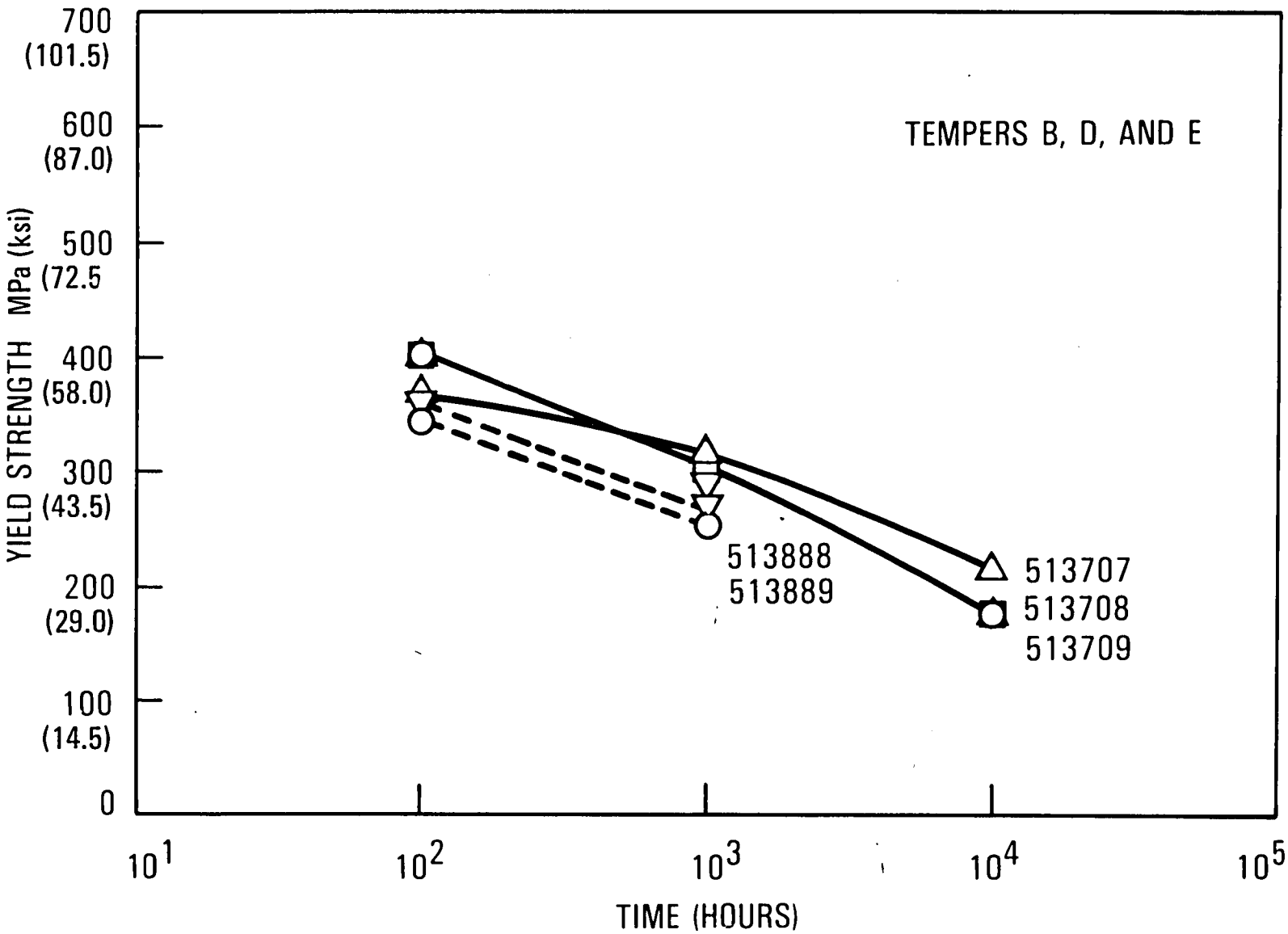

Figure 20. - Room temperature strength of P/M 2XXX Al alloys after exposure to 450 K (350°F).

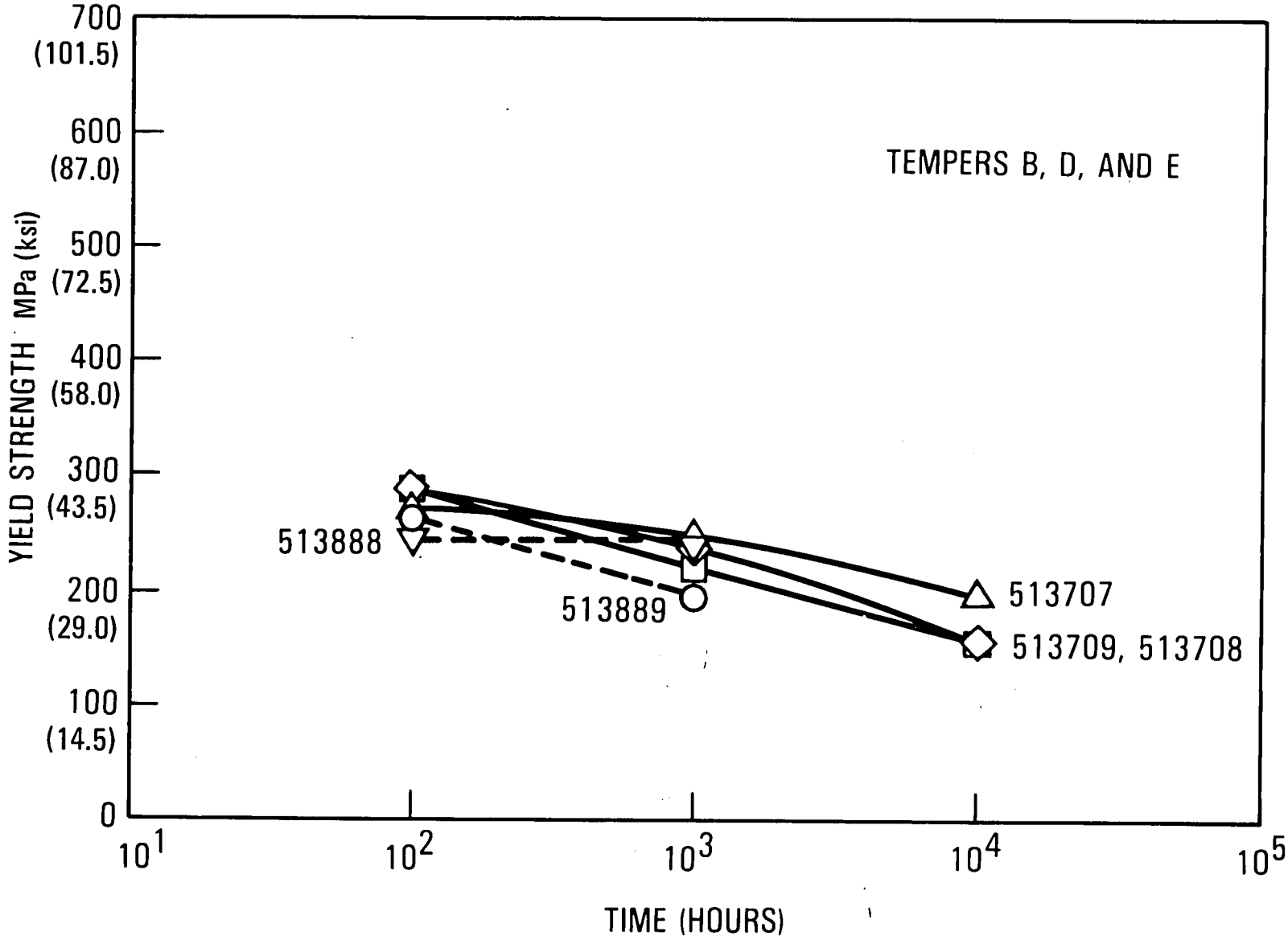

Figure 21. - Elevated temperature strength of P/M 2XXX Al alloys after exposure to 450 K (350°F).

fraction of incoherent dispersoids evaluated to date. The overall superior performance of the P/M 2618 alloy after 10,000 hours exposure suggests either a lower solute content, higher aging temperature, or both are necessary to improve the strength and stability combination after long time exposure.

4. CONCLUSIONS

1. The rapid solidification rates produced by atomization prohibit the precipitation of coarse, primary Al_3Zr in P/M 2124-Zr modified alloys that contain as much as 0.60 wt. pct. Zr. Most of the Zr forms as a finely distributed coherent Al_3Zr phase.

2. An increase in the volume fraction of dispersoid produces only a subtle decrease in grain size and degree of recrystallization in extruded P/M 2XXX Al alloys. It is suggested that this behavior may be a result of an extremely effective distribution of oxide particles in all P/M Al alloys. On an equal volume fraction basis, coherent Al_3Zr phases appear to be slightly more effective than incoherent $Al_{20}Cu_2Mn_3$ in retarding recrystallization.

3. An increase in the volume fraction of Al_3Zr, unlike $Al_{20}Cu_2Mn_3$, strengthens the P/M Al-3.70 Cu-1.85 Mg alloy without significantly reducing fracture toughness levels. An addition of 0.60 wt. pct. Zr in alloy 514042, incorporated with a 774K (935°F) solution heat treatment temperature, produced an alloy that exceeds all tensile property and fracture toughness goals for damage tolerant and fatigue resistant applications in the natural aged condition. The behavior of the P/M 2124-Zr modified alloys exceeded the properties of P/M 2124 and an experimental P/M 2124 alloy with 0.12 wt. pct. Zr.

4. The room and elevated temperature strengths after exposure to 394K (250°F) for 100, 1000 and 10,000 hours are not sensitive to the volume fraction of incoherent dispersoids present in P/M 2XXX Al alloys evaluated to date.

5. RECOMMENDATIONS FOR FUTURE WORK

1. Obtain a better understanding of the equilibrium and metastable Al-Cu-Mg-Zr phase relationships in order to minimize the loss of Cu and Mg. These alloying elements form the basis for determining the strength-fracture toughness properties available with 2XXX series Al alloys.

2. Evaluate the effect of Zr and Mn containing dispersoid phases in P/M 2124 Al alloy extrusions on elevated temperature resistance and stability, fracture toughness, and notched fatigue properties in the selected artificially aged tempers.

3. The introduction and structural application of P/M 2XXX Al alloy materials on aircraft systems is limited by the lack of established processing methods leading to plate and sheet products. The following technical objectives are recommended to alleviate this situation in a proposed follow-on effort: (a) explore the range of potential microstructural variations encountered in the fabrication of flat rolled products, and (b) establish the relationships between deformation processing conditions, alloy microstructure, and mechanical property behavior.

6. REFERENCES

1. Wald, G.G.: Supersonic Cruise Vehicle Technology Assessment Study of an Over/Under Engine Concept - Advanced Aluminum Alloy Evaluation, Final Report, NASA Contractor Report 165676, May 1981, Lockheed-California Company.

2. Chellman, D.J.; Slaughter, H.C.: Development of Powder Metallurgy 2XXX Series Al Alloys for High Temperature Aircraft Structural Applications - Phase II, Final Report, NASA Contractor Report 165965, August 1981, Lockheed-California Company.

3. Westengen, H.; Auran, L.; Reiso, O.: Effect of Minor Addition of Transition Elements on the Recrystallization of Some Commercial Aluminum Alloys, Aluminum, vol. 57, 1981 January, pp. 797-803.

4. Warlimont, H.; Necker, G.; Schultz, H.: On the Recrystallization of Doped Tungsten Wire, Z. Metall., 66, 1975, pp. 279-286.

5. Furrer, P.; Warlimont, H.: The Effect of Segregation and Precipitation on the Annealing Behavior and Grain Size of Aluminum Alloys, Aluminum, vol. 54, 1978 January, pp. 135-142.

6. Chen, C. Q.; Knott, J. F.: Effect of Dispersoid Particles on Toughness of High Strength Al Alloys, Met. Sci., vol. 15, 1981 August, pp. 357-364.

7. Ohashi, T.; Ichikawa, R.: Duplex-Precipitation Hardening in Al-Zn-Mg Alloys Highly Supersaturated with Zr, Met. Trans. A, vol. 12A, 1981 March, pp. 546-549.

APPENDIX

Identification of Tetragonal Al_3Zr by Aperture Limited Microdiffraction.

The following section lists the procedure and data used to identify the large rectangular particle in figure 22 by aperture limited microdiffraction.

Determination of camera constant

Measure R, the projected length of the diffraction vector g_{200} on the photograph, and multiply by the corresponding d_{200} where

$$Rd = \lambda L$$

$$(15.28 \text{ mm})\ (2.024\text{Å}) = 30.93 \text{ mmÅ}$$

Determine d_{hkl} for diffraction spots in pattern A and B

Pattern	Spot	R (mm)	d_{hkl} (Å)
A	1	9.4	3.29
	2	13.6	2.28
	3	8.3	3.73
B	1	8.0	3.87
	2	11.0	2.81
	3	8.1	3.81

Search for hkl with d_{hkl} from pattern A and B

Values of d_{hkl} are calculated for tetragonal $(DO_{23})Al_3Zr$ using the equation:

$$\frac{1}{d} = \frac{h^2 + k^2}{a_o^2} + \frac{l^2}{c_o^2}$$

where $a_o = 4.013$Å and $c_o = 17.321$Å. Possible hkl are identified by paring similar values of actual and measured d_{hkl}.

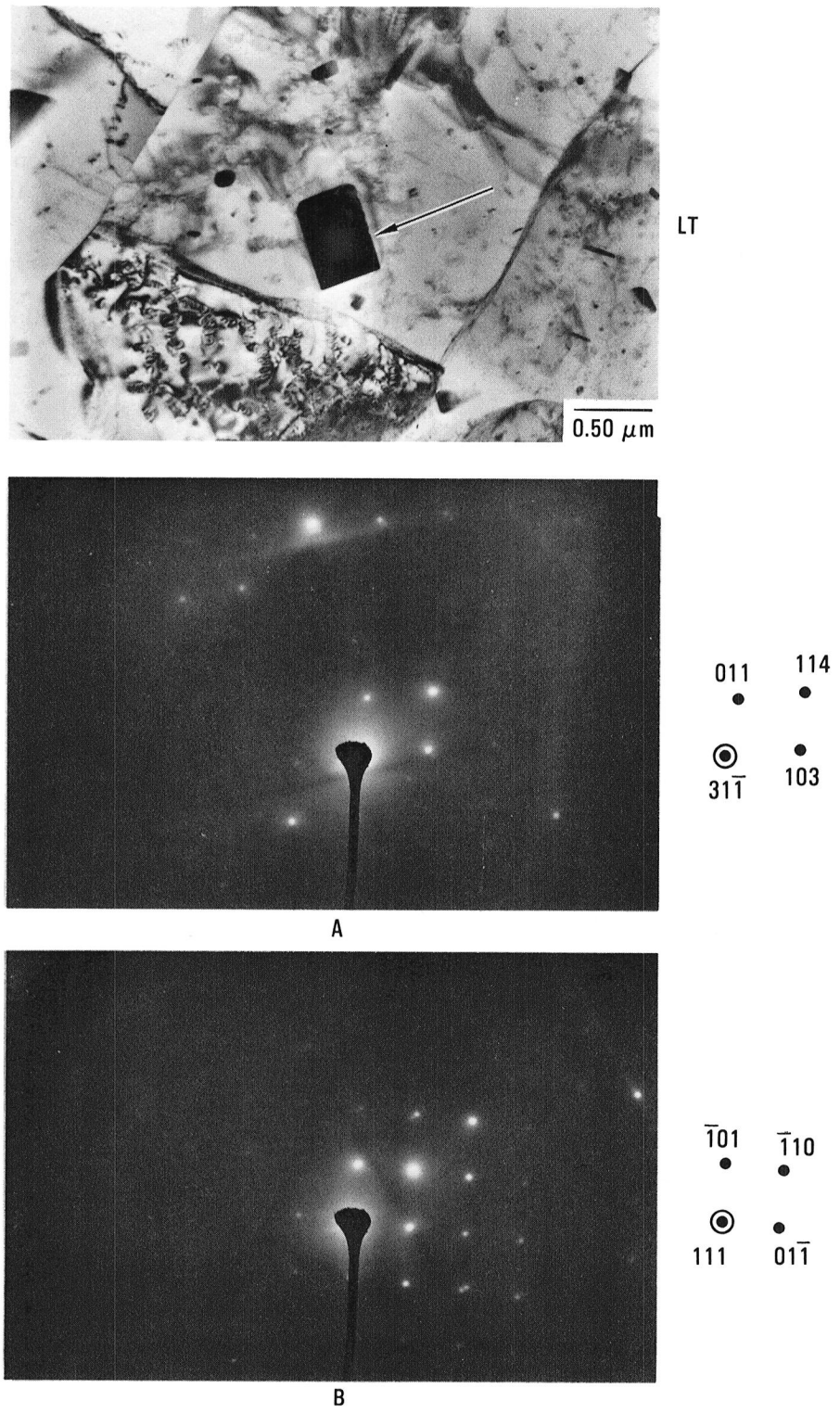

Figure 22. - Aperture limited microdiffraction patterns used to identify the rectangular shaped particles as tetragonal $(DO_{23})Al_3Zr$.

hkl	d_{hkl} Actual	d_{hkl} Measured	Pattern	Spot
001	17.32			
002	8.66			
003	5.77			
004	4.32			
010,100	4.01			
101,011	3.91	3.91,3.81,3.87	A,B,B	3,3,1
103	3.29	3.29	A	1
110	2.83	2.81	B	2
105	2.61			
114	2.37	2.28	A	2
008	2.16			
200,020	2.01			
022,202	1.95			
121,211	1.78			

Verification of indexed patterns

Before indexing pattern A and B, the interplanar angle, ϕ, was measured and verified from calculated angle using the following equation:

$$\cos\phi = \frac{\frac{h_1h_2 + k_1k_2}{a_o^2} + \frac{l_1l_2}{c_o^2}}{\left[\frac{h_1^2 + k_1^2}{a_o^2} + \frac{l_1^2}{c_o^2}\,\frac{h_2^2 + k_2^2}{a_o^2} + \frac{l_2^2}{c_o^2}\right]^{1/2}}$$

where $h_1\ k_1\ l_1$ and $h_2k_2l_2$ are the miller indices of the two diffraction spots.

Pattern	$H_1k_1l_1$	$h_2k_2l_2$	Interplanar Angle Measured	Interplanar Angle Calculated
A	101	013	81.0°	82.6°
	101	114	42.0°	45.6°
	013	114	37.0°	37.0°
B	$\bar{1}10$	$\bar{1}01$	46.0°, 47.5°	46.5°
	$\bar{1}01$	$01\bar{1}$	86.0°	87.1°

Determination of zone axis

The zone axes of pattern A and B were verified by comparing the calculated and measured interplanar angle.

Pattern A ($31\bar{1}$)
Pattern B (111)

Measured angle 33°
Calculated angle 29.7°